

# ELECTROCHEMICALLY-GRAFTED BIOTINYLATED CARBAZOLES

---

A Thesis

Presented to

the Faculty of the Department of Chemistry

University of Houston

---

In Partial Fulfillment

of the Requirements for the Degree

Master of Science

---

By

Deepali Arvind Worlikar

May 2012

## ELECTROCHEMICALLY-GRAFTED BIOTINYLATED CARBAZOLES

---

Deepali Arvind Worlikar

APPROVED:

---

Dr. Rigoberto C. Advincula, Chairman

---

Dr. Debora Rodrigues

---

Dr. Jeremy May

---

Dr. Randolph P. Thummel

---

Dr. Shoujun Xu

---

Dr. Mark A. Smith, Dean

College of Natural Sciences and Mathematics

## ACKNOWLEDGEMENTS

Firstly, I would like to express my deepest gratitude to my advisor Dr. Rigoberto C. Advincula for accepting me in his research group. His guidance and valuable advice will help me in my future endeavors. He has been an excellent mentor and has not only inspired me as a chemist, but also as someone who could be looked up to for inspiration in life.

I am deeply thankful to my lab-mate Dr. Jane Felipe for her contribution in this research project and moral support throughout. I appreciate the kind support of all my lab-mates, especially Allan C. Yago for his useful tips and guidance on this project.

I am thankful to all my committee members for their time, support, and guidance. I thank all the professors who have taught me all these years. I thank the Chemistry office staff for their support in various ways during my stay at University of Houston.

I deeply thank my beloved parents Mr. Arvind J. Worlikar and Mrs. Smita A. Worlikar; my dear siblings, Dr. Shilpa A. Worlikar, Ms Mayura A. Worlikar, and Mr. Amey A. Worlikar for their love and faith.

Last but not the least, I thank all my friends in Houston and back in India.

# ELECTROCHEMICALLY-GRAFTED BIOTINYLATED CARBAZOLES

---

An Abstract of a Thesis

Presented to

The Faculty of the Department of Chemistry

University of Houston

---

In Partial Fulfillment

of the Requirements for the Degree

Master of Science

---

By

Deepali Arvind Worlikar

May 2012

## ABSTRACT

Biotin-Streptavidin is known to be one of the strongest non-covalent interactions with dissociation constant,  $K_d \sim 10^{-15}$ . Non-specific adsorption of proteins is one of the major concerns in the design of a biosensor device which causes bio-fouling and ultimately reduces the life span of a bio-device. The main challenge in the surface functionalization for affinity-based methods is to immobilize one of the interacting compounds on the surface in such a way that nonspecific interactions of the protein with the surface are minimized. Taking into consideration the possibility of both, specific and nonspecific adsorption of streptavidin on surfaces, this study is designed to incorporate poly(ethyleneglycol) as a protein resistant functional moiety, and biotin for the formation of biotin-streptavidin bridge for protein immobilization. PEGylated carbazole compounds were first synthesized via a series of organic reactions. These compounds were further biotinylated through EDC-DMAP coupling chemistry. The biotinylated compounds were characterized by  $^1\text{H}$  NMR,  $^{13}\text{C}$  NMR, and ultraviolet-visible spectroscopy. Thin films of the biotinylated carbazole compounds were then fabricated on a quartz crystal of QCM by electrochemical deposition method. The electrodeposited films were further tested for the selective binding of streptavidin. In brief, the study aims to provide a new platform for the immobilization of streptavidin via electrochemical grafting. The ability to fine-tune the formation of a polymer film with electrochemically-controlled thickness will potentially enable the engineering of new molecular templates for biosensor applications.

## TABLE OF CONTENTS

|   |       |
|---|-------|
| Acknowledgements.....                         | iii   |
| Abstract.....                                 | v     |
| List of Figures.....                          | ix    |
| List of Schemes.....                          | x     |
| <br>Chapter 1: Introduction.....              | <br>1 |
| 1. Biosensors.....                            | 1     |
| 1.1. General Overview.....                    | 1     |
| 1.2. Biocompatibility.....                    | 2     |
| 1.2.1. Poly(ethylene glycol) on Surfaces..... | 3     |
| 1.3. Immobilization Methods.....              | 5     |
| 1.3.1. Covalent Immobilization.....           | 6     |
| 1.3.2. Non-covalent Immobilization.....       | 7     |
| 1.4. Conducting Polymers.....                 | 8     |
| 1.5. Streptavidin-Biotin Interaction.....     | 10    |
| 1.5.1. Recent Developments.....               | 12    |
| 1.6. Quartz Crystal Microbalance.....         | 14    |
| 1.6.1. Principle.....                         | 14    |
| 1.6.2. Applications.....                      | 15    |
| 1.7. Objectives of the Study.....             | 19    |
| 1.8. References.....                          | 20    |

|   |    |
|---|----|
| Chapter 2: Experimental.....  | 28 |
| 2.1. Materials.....   | 28 |
| 2.2. Characterization.....  | 28 |
| 2.3. Film Fabrication.....  | 28 |
| 2.4. Atomic Force Microscopy (AFM).....   | 30 |
| 2.5. Quartz Crystal Microbalance.....   | 30 |
| 2.6. Synthesis.....   | 31 |
| 2.6.1. Synthesis of 9-(4-Bromobutyl)-9H-carbazole.....  | 31 |
| 2.6.2. Synthesis of Toluene-4-sulfonic acid-2-[2-(2-methoxyethoxy)-ethoxy]ethyl ester.....  | 32 |
| 2.6.3. Synthesis of 3-Hydroxy-5-{2-[2-(2-methoxyethoxy)-ethoxy]-ethoxy}-benzoic acid methyl ester.....  | 33 |
| 2.6.4. Synthesis of (3-(4-Carbazol-9-yl-butoxy)-5-{2-[2-(2-methoxyethoxy)-ethoxy]-ethoxy}-benzoic acid methyl ester.....  | 33 |
| 2.6.5. Synthesis of (3-(4-Carbazol-9-yl-butoxy)-5-{2-[2-(2-methoxyethoxy)-ethoxy]-ethoxy}-phenyl)-methanol.....   | 34 |
| 2.6.6. Synthesis of 5-(2-Oxo-hexahydro-thieno[3,4-d]imidazole-4-yl)-pentanoic acid 3-(4-carbazol-9-yl-butoxy)-5-{2-[2-(2-methoxyethoxy)-ethoxy]-ethoxy}-benzyl ester..... | 35 |
| Chapter 3: Results and Discussion.....  | 37 |
| 3.1. Synthesis.....   | 38 |
| 3.2. Film Fabrication: Electrochemical Deposition.....  | 42 |
| 3.3. Streptavidin Sensing: Electrochemical Quartz Crystal Microbalance.....   | 47 |
| 3.4. References.....  | 50 |

|  |    |
|--|----|
| Chapter 4: Conclusion and Future Work.....               | 52 |
| 4.1. Conclusion.....                                     | 52 |
| 4.2. Future Work.....                                    | 53 |
| Appendices $^1\text{H}$ NMR and $^{13}\text{C}$ NMR..... | 54 |



## List of Figures

|                   |  |    |
|-------------------|--|----|
| <b>Figure 1.1</b> | Biofouling.....  | 3  |
| <b>Figure 1.2</b> | An immobilization method that controls the space around individual probe molecules.....  | 5  |
| <b>Figure 1.3</b> | Conducting polymers.....   | 9  |
| <b>Figure 3.1</b> | Molecular design of the study.....   | 38 |
| <b>Figure 3.2</b> | Cross-linking of carbazole.....  | 43 |
| <b>Figure 3.3</b> | CV traces of (a) 200 $\mu$ M, (b) 500 $\mu$ M, and (c) 1 mM biotinylated compound <b>6</b> in acetonitrile; and monomer-free scan of (d) 200 $\mu$ M, (e) 500 $\mu$ M, and (f) 1 mM solutions..... | 44 |
| <b>Figure 3.4</b> | AFM topographic images of (a) 200 $\mu$ M, (b) 500 $\mu$ M, and (c) 1 mM biotinylated compound <b>6</b> on Au substrate.....   | 46 |
| <b>Figure 3.5</b> | UV-vis spectra of electrochemically-grafted and dropcast of compound <b>6</b> on Indium Tin Oxide substrate.....   | 47 |
| <b>Figure 3.6</b> | Change in $\Delta F$ vs. time of compound <b>6</b> on a QCM crystal.....   | 48 |
| <b>Figure 3.7</b> | Change in $\Delta F$ vs. time data for the adsorption of streptavidin on a QCM crystal functionalized with biotin film.....  | 49 |

## List of Schemes

|                   |  |    |
|-------------------|--|----|
| <b>Scheme 1.1</b> | Schematic representation of a typical biosensor.....   | 2  |
| <b>Scheme 1.2</b> | Schematic representation of the immobilization of biomolecules on the polymeric self-assembled monolayers.....   | 6  |
| <b>Scheme 1.3</b> | Immobilization of streptavidin on biotin-thiol functionalized gold surface and biotin DNA assembly for subsequent target DNA hybridization.....                    | 12 |
| <b>Scheme 2.1</b> | Synthesis of PEGylated carbazole.....  | 31 |
| <b>Scheme 2.2</b> | Synthesis of biotinylated carbazole.....   | 35 |
| <b>Scheme 3.1</b> | Synthesis of 9-(4-Bromobutyl)-9H-carbazole.....  | 38 |
| <b>Scheme 3.2</b> | Synthesis of toluene-4-sulfonic acid-2-[2-(2-methoxyethoxy)-ethoxy]ethyl ester.....  | 39 |
| <b>Scheme 3.3</b> | Synthesis of 3-Hydroxy-5-{2-[2-(2-methoxyethoxy)ethoxy]ethoxy}benzoic acid methyl ester.....   | 40 |
| <b>Scheme 3.4</b> | Synthesis of (3-(4-Carbazol-9-yl-butoxy)-5-{2-[2-(2-methoxyethoxy)ethoxy]ethoxy}benzoic acid methyl ester....  | 40 |
| <b>Scheme 3.5</b> | Synthesis of (3-(4-Carbazol-9-yl-butoxy)-5-{2-[2-(2-methoxyethoxy)-ethoxy]-ethoxy}-phenyl)-methanol.....   | 41 |
| <b>Scheme 3.6</b> | Synthesis of 5-(2-Oxo-hexahydro-thieno[3,4-d]imidazole-4-yl)-pentanoic acid 3-(4-carbazol-9-yl-butoxy)-5-{2-[2-(2-methoxyethoxy)-ethoxy]-ethoxy}-benzyl ester..... | 42 |

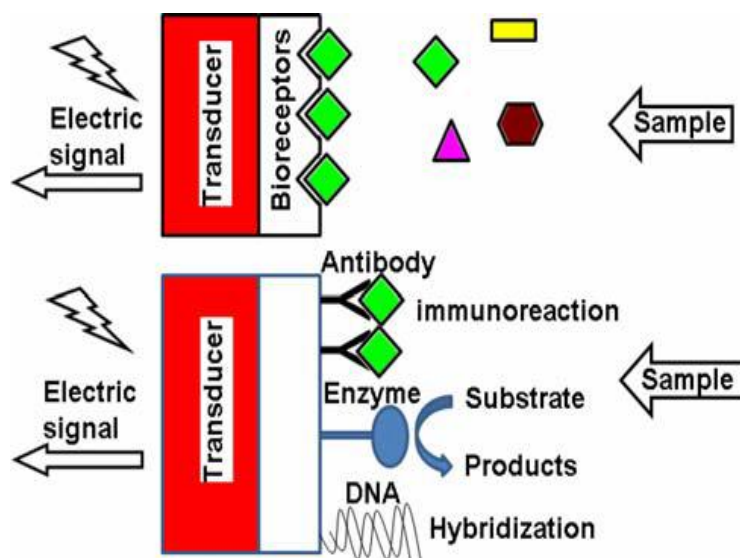
# **Chapter 1: Introduction**

## **1. Biosensors**

### **1.1. General Overview**

A biosensor is one type of a detection system that consists of a biomolecule for molecular recognition and a transducer that converts the signal arising from the interaction between an analyte and the biomolecule into another signal that can be easily analyzed, for example, an electrical signal (Scheme 1.1). All the transducers fall into four major categories namely, piezoelectric, optical, electrochemical, and thermal.<sup>1-3</sup> They are small, portable, and are suitable for detection of the analytes present in very small amounts in the solution.

Over the past few decades, there has been a great deal of interest in the development of biosensors due to their ability to detect biospecific interactions, such as peptide-antibody, DNA hybridization, and protein-protein interactions at interfaces.<sup>4-6</sup> Hence, they find applications in numerous fields like immunoassays, pharmacogenetics, forensics, drug screening, and food analysis.<sup>7-10</sup>



**Scheme 1.1** Schematic representation of a typical biosensor. (Reprinted with permission *Monastsh Chem* **2009**, 140, 891 – 899).

## 1.2. Biocompatibility

For the proper operation of a biosensor, it is important to employ a surface that is biologically inert. Usually, implantation of biomaterials is followed by non-specific adsorption of proteins that may trigger a number of unwanted responses like coagulation of blood, bacterial infection, fibrosis, inflammation, and allergy.<sup>11-13</sup> Shown in Figure 1.1 is an example of how adsorption of proteins to a surface can lead to serious problems. After proteins have adsorbed to the material, a cascade of complex events can take place. For example, if platelets adhere to the interface, they release thrombin, a protein that directs the formation of a fibrin matrix which in turn stabilizes the adsorbed cells. The large number of the proteins and cells adhered to a surface can form an aggregate called a thrombus. Finally, the thrombus can cause vascular obstruction at the place of its formation, or, even more severe can cause embolism.<sup>14</sup>

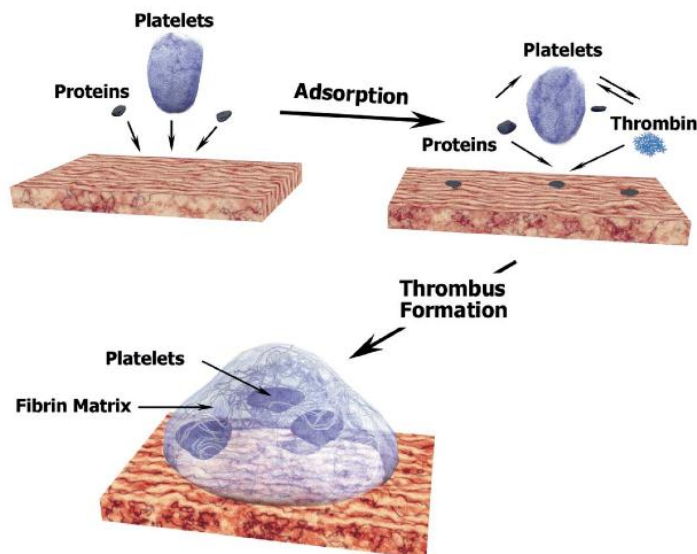


**Figure 1.1** Biofouling (Reprinted with permission *Surface Science* **2002**, 500, 61- 83).

Biofouling can have a detrimental effect on the proper functioning of an interface that is used in biosensing applications — initially it degrades the performance of the biodevices and ultimately reduces their lifespan. It is therefore important to eliminate or at least reduce non-specific adsorptions for the proper functioning of these biodevices.<sup>15-</sup>

16

### 1.2.1. Poly(ethylene glycol) on Surfaces

Various materials have been studied in the past for their protein resistance; however, only a few of them were able to significantly reduce nonspecific protein adsorption. Some of these materials include polysaccharides<sup>17</sup>, dextran<sup>18</sup>, cellulose dialysis membranes<sup>18</sup>, zwitterionic compounds<sup>19</sup>, and poly(ethylene glycol) (PEG)<sup>20</sup>. In

particular, PEG has been extensively used due to its inertness to cell and protein adhesion, good biocompatibility, low toxicity, non-immunogenicity, and high water solubility.<sup>21-22</sup>

PEG is an amphiphilic polyether that is usually incorporated to a surface to minimize protein adsorption. For decades, the non-fouling property of PEG towards proteins has received much attention. Understanding the molecular mechanisms leading to its protein resistance is very important since different molecular mechanisms may be involved. Prime and Whitesides showed that short oligo(ethylene glycol) chains with just three repeating units in helical or amorphous forms were capable of resisting non-specific protein adsorption. They illustrated that the presence of flexible PEG strands is necessary for protein resistance.<sup>23</sup> The protein resistance is due to the prevention of the direct interaction between the surface and the protein by forming a stable solid-liquid interface involving tightly bound water. Quantum calculations by Grunze also suggested that the densely-packed all-trans phase of PEG terminated SAM cannot form a stable solvation layer, while the helical structure stabilizes such a layer.<sup>24</sup> On the other hand, Szleifer showed that the presence of a dense and inert film prevents contact between the substrate and the protein rendering the film protein-resistant.<sup>25</sup>

From the above theories, it is clear that grafting density affects PEG's ability to resist proteins. Thus, the manipulation of the architecture of a resistant film is necessary to effectively control their degree of protein non-specific adsorption.

### 1.3. Immobilization Methods

Surfaces with immobilized biologically active molecules like proteins<sup>26</sup>, DNA<sup>27</sup>, peptides<sup>28</sup>, and sugars<sup>29</sup> are useful for studying biomolecular interactions. For these studies, not only a high density of biomolecules on the surface is required but these biosurfaces should be capable of minimizing steric hindrance and preventing non-specific adsorptions for efficient and sensitive biospecific interactions<sup>30</sup>. Moreover, the structure and activity of the ligand should be retained on immobilization.<sup>31</sup>

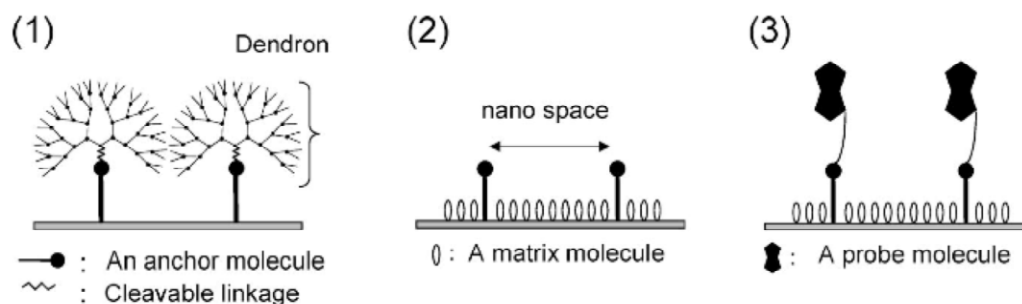
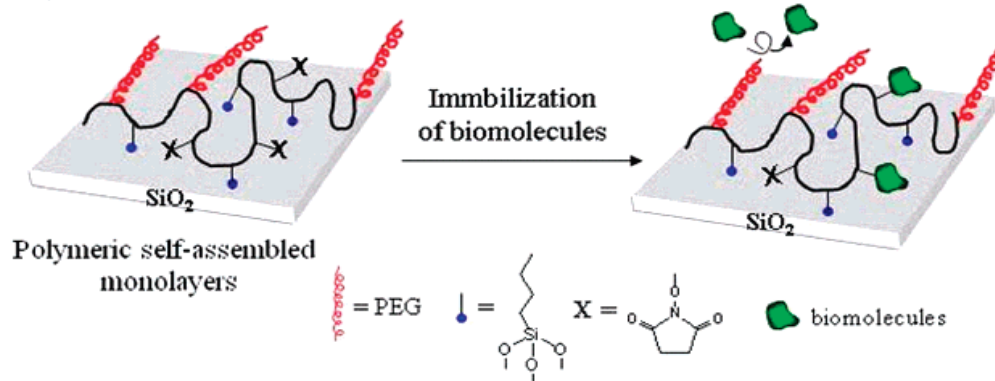


**Figure 1.2** An immobilization method that controls the space around individual probe molecules. (Reprinted with permission *Langmuir* **2009**, 25, 1633.)

From these criteria, it is imperative that a rational design for a good biosensor involves a method of good immobilization of the biological recognition molecule on the sensor surface. Various ways of grafting biomolecules on surfaces reported in the literature include non-covalent, covalent, entrapment, and encapsulation methods.<sup>32</sup>

### 1.3.1. Covalent Immobilization

Covalent immobilization techniques make use of different functional groups present on the biomolecules that are not necessary for their biological activity for their covalent binding to the modified surfaces. One of the most popular methods for the covalent immobilization of biomolecules is through formation of self-assembled monolayers (Scheme 1.2).



**Scheme 1.2** Schematic representation of the immobilization of biomolecules on the polymeric self-assembled monolayers (Reprinted with permission *Langmuir* **2007**, 23, 10902 – 10905)

For example, Engin *et al.* employed a self-assembled monolayer of benzylguanine thiol for the covalent attachment of SNAP-tag fusion protein<sup>33</sup>. Covalent immobilization can also be achieved through the formation of an amide bond between the amine group on the biomolecule and the surfaces modified with esters like *N*-hydroxysuccinimide (NHS). However, NHS esters are unstable in aqueous conditions and can undergo hydrolysis. An alternative method is by employing an epoxide functionalized surface



since epoxides are relatively stable to hydrolysis under neutral pH conditions. Another approach for the covalent attachment of biomolecules is through formation of an imine by a coupling reaction between an aldehyde present on the surface and a primary amine group of the biomolecule.<sup>34</sup> The imine can be further reduced to a secondary amine. Proteins bearing thiol groups can be covalently attached to maleimide modified surfaces via formation of thioether bonds.<sup>35</sup> MacBeath *et al.* demonstrated immobilization of small molecules like biotin and pipicolyl  $\alpha$ -ketoamide on a glass substrate via coupling thiol to the surface-bound maleimide groups.<sup>36</sup>

### **1.3.2. Non-covalent Immobilization**

Non-covalent immobilization is achieved through a reversible interaction between the biomolecule and the surface through Van der Waals forces, electrostatic forces, ionic and hydrogen bonds, and hydrophobic bonding.<sup>32</sup> Hydrophobic adsorption is carried out using either polystyrene microtiter plates or nitrocellulose membranes whereas polylysine coated slides are used for electrostatic binding.<sup>35</sup> This method of immobilization does not require any coupling reagents nor any modification strategies for the biomolecules to be immobilized. Mahoney *et al.* demonstrated a method for non-covalent immobilization of heparin onto microtiter wells for the detection of heparin-binding proteins like TSC-6, chemokines IL-8 and KC, and complement factor H.<sup>37</sup> There are several other reports in the literature concerning the non-covalent adsorption of proteins on surfaces.<sup>38-40</sup> However, these interactions are not very stable and suffer from severe drawbacks. The reversible nature of these interactions can cause the leaching of proteins from the support

thus contaminating the surrounding media.<sup>41</sup> These interactions are not as robust as the covalent interactions and may cause denaturation of the proteins on adsorption.<sup>42</sup> Moreover, since there is no control over the orientation and packing density of the immobilized biomolecules, there might be a further reduction in their activity due to steric hindrance.<sup>43</sup>

#### **1.4. Conducting Polymers**

The last few decades have experienced a growing interest in the study of conducting polymers. Several studies have been reported in the literature describing the synthesis, properties, and potential applications of conducting polymers such as polythiophene<sup>44-46</sup>, polyaniline<sup>47-48</sup>, and polypyrrole<sup>49-50</sup> (Figure 1.3). Some of these applications include solar cells, sensors, light emitting diodes, batteries, and corrosion protection.<sup>51-55</sup> Conducting polymers can be synthesized by electrochemical methods. This technique has the following advantages<sup>56</sup>: (a) These materials can be produced on the electrode surface itself and can be further characterized by electrochemical and/or spectroscopic methods. (b) The thickness of the film can be easily controlled by varying the parameters like potential or current during the deposition.

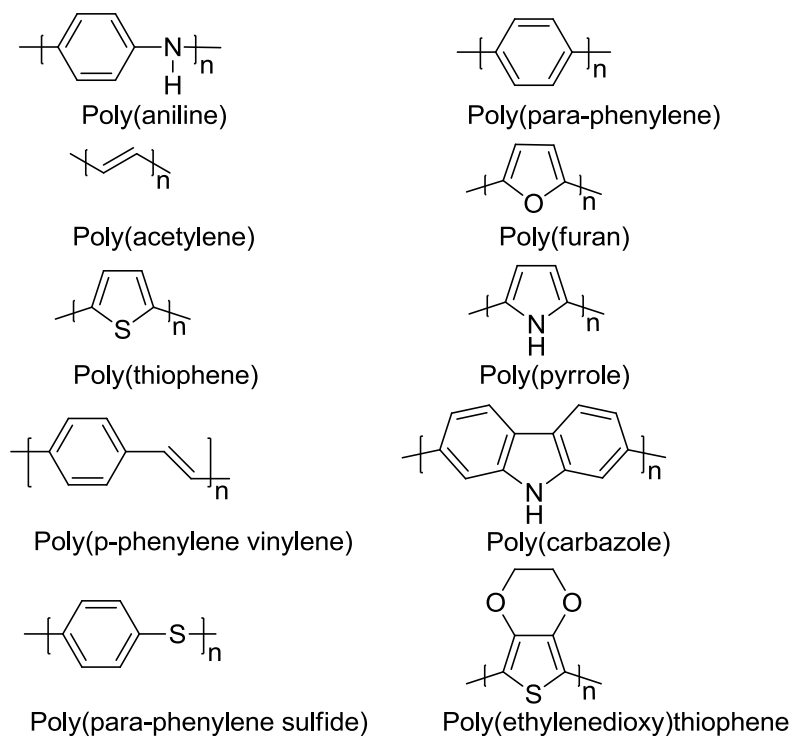


**Figure 1.3** Conducting polymers

Previously, our group has demonstrated the precursor polymer approach for the deposition of conjugated polymers on conducting substrates. The precursor polymer with an electroactive pyrrole moiety was first synthesized by free-radical polymerization and then electropolymerized on the conducting substrate. The *inter*- and *intra*-molecular polymerization resulted in a cross-linked polymer film which can be investigated for its electro-optical properties.<sup>57</sup> We have also reported electropolymerization, cross-linking, and ultrathin film formation of polymethylsiloxane-modified polythiophene precursor polymers.<sup>58</sup> Carbazole bearing polymers have been extensively studied in our group.<sup>59-60</sup> Recently, we developed bioresistant coatings of OEGylated carbazole dendrons which can be electrodeposited on gold or any other conducting substrates by electropolymerization of the carbazole functionality.<sup>61</sup> Moreover, we have reported a

number of studies on carbazole containing dendrimers and dendrons that can be electropolymerized.<sup>62-65</sup>

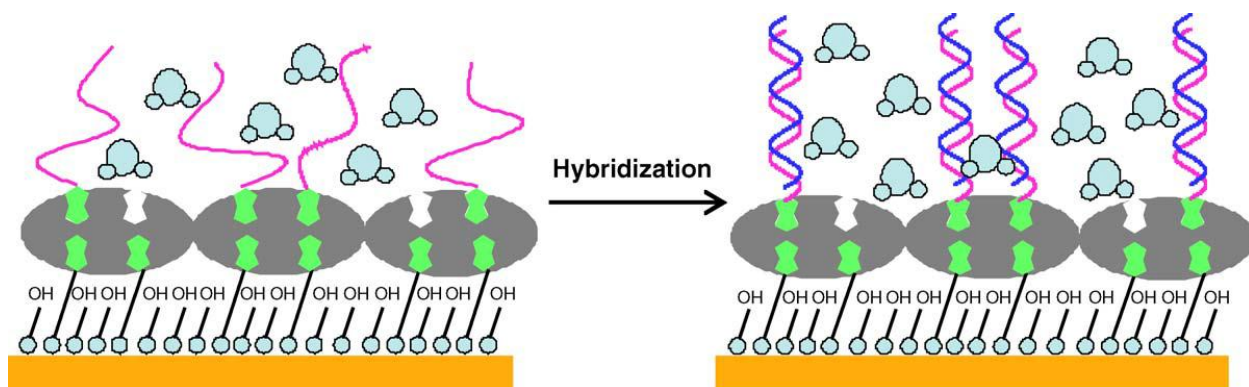
In our present study, we have introduced PEGylated carbazole for the electrochemical deposition of biotin on gold surfaces for subsequent streptavidin sensing. This is an efficient method for immobilization of ligands onto the surfaces as compared to other methods previously reported since it may enable a better control over the density of the ligands on the surface. In biotin-streptavidin sensing, it is important to have correct amount of biotin on the surface for the efficient capture of streptavidin. Through electrochemical deposition we can have control over the thickness of biotin film on the substrate by just varying the current or potential during deposition. Moreover, it is not limited to gold substrates but is applicable to any other conducting substrates.

### **1.5. Streptavidin-Biotin Interaction**

Avidin is a tetrameric protein which does not undergo denaturation even in presence of 8M urea or 3M guanidine hydrochloride. It's interaction with a small vitamin biotin is known to be one of the strongest non-covalent interaction which makes it an ideal candidate in bioconjugate chemistry. The avidin-biotin complex is stable under extreme conditions like high temperatures, presence of denaturants and requires a minimum of 3M guanidine at pH 1.5 to induce complete dissociation of the complex. The biotin-avidin interaction is similar to antibody-antigen or receptor-ligand recognition but with much higher affinity constants. However, due to its high isoelectric point (pI) and

carbohydrate content, it can bind to molecules other than biotin. This non-specific behavior of avidin can be overcome by another biotin binding protein streptavidin.<sup>66</sup>

Streptavidin is a tetrameric protein which is extracted from *Streptomyces avidinii*. It has a very high affinity for biotin with  $K_d \sim 10^{-15}$ . The molecular mass of streptavidin is about 60,000 D which is slightly greater than avidin. The primary structure of streptavidin is completely different from that of avidin in the sense that they have different amino acid sequence. The isoelectric point of streptavidin (pI 5-6) is much lower than that of avidin (pI 10) which plays a significant role in the reduction of non-specific bindings.<sup>66</sup> With four biotin binding sites, a single molecule of streptavidin can bind up to four molecules of biotin.<sup>67</sup> These biotin binding sites are located on two opposite sides of the protein.<sup>68</sup> Due to its dyad symmetry, streptavidin can bind to a biotinylated surface while exposing the other two biotin binding sites to the aqueous phase. These biotin binding sites can be further used for the immobilization of other biotinylated moiety.<sup>69</sup> (Scheme 1.3)



**Scheme 1.3** Immobilization of streptavidin on biotin-thiol functionalized gold surface and biotin DNA assembly for subsequent target DNA hybridization [reprinted with permission *Biosens. Bioelectron.* **2005**, 21, 719.]

In biodevices, site-specific immobilization of proteins is crucial in order to maintain their biological activity. A biotinylated surface is an ideal platform since biotin-streptavidin is known to be one of the strongest non-covalent biomolecular interaction.<sup>70</sup> Streptavidin is a very stable protein that can withstand extreme harsh conditions like high temperatures, high concentrations of denaturants and organic solvents while still maintaining its molecular structure.<sup>71</sup>

### 1.5.1. Recent Developments

The biotin-streptavidin interaction chemistries have been exploited by a number of research groups. Huang *et al.* employed a biotin-derivatized poly(L-lysine)-g-poly(ethylene glycol) copolymer for the immobilization of streptavidin on niobium oxide

surfaces. This system was further used for the binding of biotinylated goat antirabbit immunoglobulin ( $\alpha$ RIgG-biotin) as a capture molecule in order to sense the rabbit immunoglobulin (RIgG) target molecule.<sup>72</sup> Azzaroni *et al.* demonstrated the supramolecular bioconjugation of streptavidin on a biotinylated self-assembled monolayer (SAM) of biotin-terminated thiol and 11-mercapto-1-undecanol. This system was then monitored for the reorganization of the streptavidin layer which takes place within the biotinylated film.<sup>68</sup> Kim *et al.* reported a high-sensitive biomolecule detection technique in which a gold surface was modified with biotin and then subsequently functionalized with biotinylated gold nanoparticles through a streptavidin bridge.<sup>73</sup> Yang and coworkers introduced a novel method called microstamping onto an activated polymer surface (MAPS) to pattern biotin on carboxylic acid derivatized poly(ethylene terephthalate) (PET) followed by its subsequent binding with streptavidin.<sup>74</sup> Hyun and coworkers applied the same method to check the feasibility of creating biotin and streptavidin micropatterns on other polymeric materials like polyethylene (PE), polystyrene (PS), poly(methyl methacrylate) (PMMA), and PET since these materials are commonly used as biomaterials and in tissue culture.<sup>75</sup> In an another approach, Hook *et al.* used biotin-modified supported lipid bilayers on SiO<sub>2</sub> for the immobilization of streptavidin followed by the sequential coupling of single stranded biotinylated DNA for subsequent DNA immobilization.<sup>76</sup> Gronewold and co-workers covalently attached a carboxymethylated dextran layer with streptavidin. This streptavidin modified surface was employed to attach biotinylated oligonucleotide capture probes to detect the BRCAI gene.<sup>77</sup>

## 1.6. Quartz Crystal Microbalance

The signal transduction mechanism of the QCM technique is based on the piezoelectric effect which was first discovered by Jacques and Pierre Curie in 1880. The Curie brothers found out that when a quartz crystal is subjected to a mechanical stress, a proportional voltage is created.<sup>78</sup> The word piezoelectricity is derived from Greek word piezin which means to press and the electricity that is generated due to this pressure. Lord Rayleigh showed that the change in inertia of the vibrating crystal changes the frequency of the crystal. Good crystal stability can be achieved by using electric resonators and room-temperature stable AT-cut crystals. In 1959, QCM was used for sensing for the first time when Sauerbray established a linear relationship between the change in mass and frequency. QCM was first used for gas-phase sensing. Later in 1980s, solution based QCM sensors were developed.

### 1.6.1. Principle:

In 1959, Sauerbrey demonstrated that there is a linear relationship between the change in the frequency of the oscillating quartz crystal and the change in mass on the surface of the crystal. When voltage is applied to a quartz crystal, it starts oscillating at a certain frequency, and the change in frequency is related to the change in the surface mass of the crystal by a well-known Sauerbrey equation:

$$\Delta F = \frac{-2F_q^2 \Delta m}{A \sqrt{\rho_q \mu_q}}$$



where  $\Delta F$  is the change in frequency of the oscillating quartz crystal,  $\Delta m$  is the change in the mass,  $n$  is the overtone number,  $A$  is the surface area of the electrode,  $\mu_q$  is a shear modulus ( $\mu_q = 2.947 \times 10^{11} \text{ g cm}^{-1} \text{ s}^{-2}$ ), and  $\rho_q$  is the density of the quartz ( $\rho_q = 2.648 \text{ g cm}^{-3}$ ). The negative sign in the above equation indicates that an increase in mass is accompanied by a decrease in frequency. However, the linear relationship holds true only when certain criteria are met. Firstly, the equation becomes invalid when the change in mass exceeds 2 % of the crystal mass. Thus, the amount of mass adsorbed onto the quartz crystal should be smaller than the mass of the quartz crystal itself. Secondly, it is applicable only to rigid elastic and rigid films since they do not dissipate energy during vibration. It does not work for viscoelastic or soft films, since they do not couple well with the oscillating crystal which causes dampening of the frequency and hence a lower shift in frequency than expected. Thirdly, the adsorbed mass should be uniformly distributed over the working area of the quartz crystal.<sup>79-81</sup>

### **1.6.2. Applications:**

A number of techniques like fourier transform infrared (FTIR) spectrometry, gas chromatography (GC), and mass spectrometry (MS) are available for accurate and precise determination of the analytes. These techniques, however, are time consuming and expensive. Due to its high sensitive, low cost, portability, and selectivity, QCM is widely used in sensor applications. The success of the QCM sensors depends on the proper choice of the coating material for the detection of analytes. It is used in a plethora of applications, some of which are discussed below.<sup>82</sup>

#### **1.6.2.1. Gas Phase Detection**

In 1964, King developed a coated piezoelectric quartz crystal to detect and measure the composition of vapors and gases. These detectors were found to be highly sensitive, rugged, and fast. They were sensitive to 0.1 ppm moisture and could detect xylene as low as 1 ppm. These detectors can be made specific for certain vapors and are now commercialized as water vapor detectors.<sup>83</sup> In 1983, Guilbault was the first one to employ an enzyme for detection of substrates directly in the gas phase. He used a formaldehyde coated piezoelectric quartz crystal along with the cofactors reduced glutathione and nicotinamide adenine dinucleotide to determine the concentration of aldehyde. This detector showed an excellent selectivity to formaldehyde and showed a little response to other aldehydes or alcohols (> 1000:1 selectivity ratio at 1 and 10 ppm formaldehyde).<sup>84</sup>

#### **1.6.2.2. Immunosensors**

QCM-based immunosensors make use of antibody-coated crystals and exhibit an inherent bioselectivity.<sup>85</sup> They depend on the antibody-antigen interaction for the molecular recognition. Immunosensors can detect small molecules as well as large biomolecules. Nakamura *et al.* developed a highly sensitive sensor using an oligopeptide and a piezoelectric QCM for the detection of low molecular weight compounds under aqueous conditions. They formed a self-assembled monolayer of the peptide on the gold electrode of the quartz crystal to capture porphyrin as the target molecule. This method

showed a broad detection range from 10 ng/ml to 100 µg/ml.<sup>86</sup> Samoylov *et al.* designed a peptide biosensor based on phage display-derived peptides for the detection of peptide-cell surface marker interactions. The peptide was first immobilized on the QCM surface via biotin-streptavidin interaction. When exposed to muscle and control (kidney, liver, brain), it showed a strong response to murine muscle. A response with same  $K_d$  but lower amplitude was observed for feline muscle homogenates which indicates cross-species affinity. However, it did not show any response to murine kidney, liver, and brain homogenates for any given concentration of the homogenates. Such a biosensor can be used in clinical applications.<sup>87</sup>

#### **1.6.2.3. Detection of Drugs**

QCM has been widely used to detect drugs like paracetamol<sup>88</sup>, caffeine<sup>89</sup>, phenacetin<sup>90</sup>, sialic acid<sup>91</sup>, procainamide<sup>92</sup>, o-phenylenediamine<sup>93</sup>, and trimethoprim<sup>94</sup> over concentrations ranging from nM to mM and µM. Attili *et al.*<sup>95</sup> and Halamek *et al.*<sup>96</sup> developed a piezoelectric crystal immunosensor for the detection of cocaine. The gold electrodes of a 10 MHz piezoelectric crystal were precoated with protein G and were further coated with benzoylecgonine which is a cocaine metabolite. This sensor was used for the detection of cocaine in the concentration range 10-300 µg/litre (part per billion) with a relative SD of 10-19%. Wei *et al.* demonstrated the use of a piezoelectric crystal sensor for the detection of atropine sulfate in a pharmaceutical compound. The frequency response of the crystal was linearly proportional to the concentration of drugs and the sensor was capable of detecting the drugs present in low concentrations. The same

authors developed another piezoelectric quartz crystal sensor for the simultaneous determination of atropine sulfate and sodium chloride in atropine sulphate eye drops in which they employed one separated electrode which could be immersed in liquid.<sup>97</sup> In another approach, a swellable styrene-divinylbenzene copolymer was immobilized on a quartz crystal for the detection of an antibiotic cefoperazone. A large change in frequency corresponding to the analyte concentration was observed which finds application in designing thickness-shear mode (TSM) acoustic wave sensor.<sup>98-99</sup>

#### **1.6.2.4. Cell-based QCM Biosensors**

For cell-based QCM biosensors, the cells must be adherent to the QCM surface. Normal eukaryotic cells attach to the surface through their internal cytoskeleton. In order to initiate this attachment process, the cells need a sufficiently hydrophilic surface. The gold surface of the QCM crystal is moderately hydrophobic and thus not suitable for the attachment of cells. These surfaces need to be modified and made more hydrophilic.<sup>100-103</sup> Fredriksson *et al.* modified the QCM surface with polystyrene by spin-coating method. The hydrophobic polystyrene coated surface was then subjected to a UV/ozone treatment to make it hydrophilic and thus favorable for cell adhesion. These crystals were then used for *in vitro* real-time characterization of cell attachment and spreading on surfaces. The QCM response was found to be highly sensitive to very small amounts of cells and was highly specific to the chemical properties of the surface.<sup>104</sup> Marx *et al.* employed endothelial cells to investigate the effect of varying concentrations of nocodazole, a microtubule binding and disrupting drug, on the adherent cells.<sup>105</sup>

### **1.7. Objectives of the Study**

The overall objective of this study is to create a molecular template for the immobilization of streptavidin suitable for various substrates and a novel template that can give a control of the density of biotin moieties on the surface. Specifically, this study is aimed at (1) synthesizing a biotinylated compound that can be deposited electrochemically and has the ability to enhance biotin-streptavidin interaction by minimizing non-specific adsorption; (2) fabricating biotinylated film through electrochemical deposition; and (3) investigating biotin-streptavidin binding through quartz crystal microbalance technique.

## 1.8. References

- 1) Campbell, R. E. *Anal. Chem.* **2009**, 81(15), 5972.
- 2) Eggins, B. *Chemical sensors and biosensors. Analytical techniques in the sciences*; Wiley: West Sussex, 2002.
- 3) Wagner, G., Guilbault, G. G. *Food biosensor analysis*; Marcel Dekker: New York, 1994.
- 4) Wilson, D. S.; Nock, S. *Angew. Chem., Int. Ed.* **2003**, 42, 494.
- 5) Cretich, M.; Damin, F.; Pirri, G.; Chiari, M. *Biomol. Eng.* **2006**, 23, 77.
- 6) Gerhold, D.; Rushmore, T.; Caskey, C. T. *Trends Biochem. Sci.* **1999**, 24, 168.
- 7) Hermanson, G. T. *Bioconjugate techniques*; Academic Press: SanDiego, 1996.
- 8) Singh, P.; Sharma, B. P.; Tyle, P. *Diagnostics in the year 2000:antibody, biosensor, and nucleic acid technologies*; Van Nostrand Reinhold: New York, 1993.
- 9) Blum, L. J.; Coulet, P. R. *Biosensor principles and applications*; Marcel Dekker: New York, 1991.
- 10) Zapp, E.; Brondani, D.; Vieira, I. C.; Dupont, J.; Scheeren, C. W. *Electroanalysis* **2011**, 23(5), 1124.
- 11) Benhabbour, S. R.; Sheardown, H.; Adronov, A. *Macromolecules* **2008**, 41, 4817.
- 12) Anderson, J. M.; Rodriguez, A.; Changb, D. T. *Semin. Immunol.* **2008**, 20, 86.
- 13) Dee, K. C.; Puleo, D. A.; Bizios, R. *An introduction to tissue-biomaterial interactions*; John Wiley & Sons, Inc.: Hoboken, NJ, 2002.

- 14) Kim, Y. H.; Park, K. D.; Han, D. K.; Salamone, J. C. *Blood compatible polymers*; CRC Press LLC: Chicago, IL, 1998.
- 15) Li, L.; Chen, S.; Zheng, J.; Ratner, B. D.; Jiang, S. *J. Phys. Chem. B* **2005**, *109*, 2934.
- 16) Lee, B. S.; Chi, Y. S.; Lee, K.; Kim, Y. G.; Choi, I. S. *Biomacromolecules* **2007**, *8*, 3922.
- 17) McArthur, S. L.; Mclean, K. M.; Kingshott, P.; St John, H. A. W.; Chatelier, R. C.; Griesser, H. J. *Colloids Surf., B* **2000**, *17*, 37.
- 18) Österberg, E.; Bergström, K.; Holmberg, K.; Schuman, T. P.; Riggs, J. A.; Burns, N. L.; Van Alstine, J. M.; Harris, J. M. *J. Biomed. Mater. Res.* **1995**, *29*, 741.
- 19) Holmlin, R. E.; Chen, X.; Chapman, R. G.; Takayama, S.; Whitesides, G. M. *Langmuir* **2001**, *17*, 2841.
- 20) Prime, K. L.; Whitesides, G. M. *J. Am. Chem. Soc.* **1993**, *115*, 10714.
- 21) Alcantar, N. A.; Aydil, E. S.; Israelachvili, J. N. *J. Biomed. Mater. Res.* **2000**, *51*, 343.
- 22) Harris, J. M. *Poly(ethylene glycol) Chemistry: Biotechnical and biomedical applications*; Plenum Press: New York, 1992.
- 23) Prime, K. L.; Whitesides, G. M. *Science* **1991**, *252*, 1164.
- 24) Harder, P.; Grunze, M.; Dahint, R. *J Phys Chem B* **1998**, *102*, 426.
- 25) Szleifer, I. *Curr Opin Solid State Mater Sci* **1997**, *2*, 337.
- 26) Camarero, J. A.; Kwon, Y.; Coleman, M. A. *J. Am. Chem. Soc.* **2004**, *126*, 14730.
- 27) Du, H.; Strohsahl, C. M.; Camera, J.; Miller, B. L.; Krauss, T. D. *J. Am. Chem. Soc.* **2005**, *127*, 7932.

- 28) Su, J.; Bringer, M. R.; Ismagilov, R. F.; Mrksich, M. *J. Am. Chem. Soc.* **2005**, *127*, 7280.
- 29) Houseman, B. T.; Mrksich, M. *Chem. Biol.* **2002**, *9*, 443.
- 30) Hong, M.; Yoon, H. C.; Kim, H. *Langmuir* **2003**, *19*, 416.
- 31) Gujraty, K. V.; Ashton, R.; Bethi, S. R.; Kate, S.; Faulkner, J. C.; Jennings, G. K.; Kane, R. S. *Langmuir* **2006**, *22*, 10157.
- 32) Potyrailo, R.; Mirsky, V. *Combinatorial methods for chemical and biological sensors*; Springer, 2009.
- 33) Engin, S.; Trouillet, V.; Franz, C. M.; Welle, A.; Bruns, M.; Doris, W. *Langmuir* **2010**, *26*(9), 6097.
- 34) MacBeath, G.; Schreiber, S. L. *Science* **2000**, *289*, 1760.
- 35) Wong, S. L.; Khan, F.; Micklefield, J. *Chem. Rev.* **2009**, *109*, 4025.
- 36) MacBeath, G.; Koehler, A. N.; Schreiber, S. L. *J. Am. Chem. Soc.* **1999**, *121*, 7967.
- 37) Mahoney, D. J.; Whittle, J. D.; Milner, C. M.; Clark, S. J.; Mulloy, B.; Buttle, D. J.; Jones, G. C.; Day, A. J.; Short, R. D. *Anal. Biochem.* **2004**, *330*, 123.
- 38) Blum, L. J.; Gautier, S. M.; Coulet, P. R. *J. Biotechnol.* **1993**, *31*, 357.
- 39) Bengali, Z.; Pannier, A. K.; Segura, T.; Anderson, B. C.; Jang, J. H.; Mustoe, T. A.; Shea, L. D. *Biotechnol. Bioeng.* **2005**, *90*, 290.
- 40) Hilal, N.; Kochkodan, V.; Nigmatullin, R.; Goncharuk, V.; Al-Khatib, L. *J. Membr. Sci.* **2006**, *268*, 198.
- 41) Khan, F.; He, M.; Taussig, M. J. *Anal. Chem.* **2006**, *78*, 3072.
- 42) Butler, J. E. *Methods* **2000**, *22*, 4.



- 43) Kusnezow, W.; Hoheisel, J. D. *J. Mol. Recognit.* **2003**, *16*, 165.
- 44) Kaneto, K.; Yoshino, K.; Inuishi, Y. *Jpn. J. Appl. Phys.* **1982**, *21*, 567.
- 45) Garnier, F.; Tourillon, G.; Gazard, M.; Dubois, J. C. *J. Electroanal. Chem.* **1983**, *148*, 299.
- 46) Roncali, J. *Chem. Rev.* **1997**, *97*, 173.
- 47) Noufi, R.; Nozik, A. J, White, J.; Warren, L. F. *J. Electrochem. Soc.* **1982**, *129*, 2261.
- 48) Diaz, A. F.; Castillo, J. I.; Logan, J. A.; Lee, W. Y. *J. Electroanal. Chem.* **1980**, *129*, 111.
- 49) Diaz, A. F.; Kanazawa, K. K.; Gardini, G. P. *J. Chem. Soc., Chem. Commun.* **1979**, 635.
- 50) Kanazawa, K. K.; Diaz, A. F.; Gill, W. D.; Grant, P. M.; Street, G. B.; Gardini, J. P.; Kwak, J. F. *Synth. Met.* **1980**, *1(3)*, 329.
- 51) Grimaldo, E.; Hachey, S.; Cameron, C. G.; Freund, M. S. *Macromolecules* **2007**, *40*, 7166.
- 52) Zhou, Y.; Zhang, F.; Tvingstedt, K.; Barrau, S.; Li, F.; Tian, W.; Inganäs, O. *Appl. Phys. Lett.* **2008**, *92*, 233308.
- 53) Zaumseil, J.; Friend, R. H.; Sirringhaus. *Nat. Mater.* **2006**, *5*, 69.
- 54) Miller, J. S. *Adv. Mater.* **1993**, *5*, 671.
- 55) Ahmad, N.; MacDiarmid, A. G. *Synth. Met.* **1996**, *78*, 103.
- 56) Yavuz, O.; Berlouis, L. E. A.; Hitchman, M. L.; Sarac, A.S. *Synth. Met.* **2000**, *110*, 165.
- 57) Deng, S.; Advincula, R. C. *Chem. Mater.* **2002**, *14*, 4073.

- 58) Xia, C.; Fan, X.; Park, M.; Advincula, R. C. *Langmuir* **2001**, *17*, 7893.
- 59) Baba, A.; Onishi, K.; Knoll, W.; Advincula, R. C. *J. Phys. Chem. B* **2004**, *108*, 18949.
- 60) Taraneekar, P.; Baba, A.; Fulghum, T. M.; Advincula, R. C. *Macromolecules* **2005**, *38*, 3679.
- 61) Felipe, M. J.; Dutta, P.; Pernites, R.; Ponnampati, R.; Advincula, R. C. *Polymer*. **2012**, *53*, 427.
- 62) Albrecht, Ken.; Pernites, R.; Felipe, M. J.; Advincula, R. C.; Yamamoto, K. *Macromolecules* **2012**, *45*, 1288.
- 63) Taraneekar, Prasad.; Fulghum, T.; Patton, Derek.; Ponnampati, R.; Clyde, G.; Advincula, R. *J. Am. Chem. Soc.* **2007**, *129*, 12537.
- 64) Jiang, G.; Ponnampati, R.; Pernites, R.; Grande, C. D.; Felipe, M. J.; Foster, E.; Advincula, R. *Langmuir* **2010**, *26*(22), 17629.
- 65) Felipe, M. J.; Estillore, N.; Pernites, R. B.; Nguyen, T.; Ponnampati, R.; Advincula, R. C. *Langmuir* **2011**, *27*, 9327.
- 66) Hermanson, G. T. *Bioconjugate techniques*; Academic Press: San Diego, 1996.
- 67) Su, X.; Wu, Y.-J.; Robelek, R.; Knoll, W. *Langmuir* **2005**, *21*, 348.
- 68) Azzaroni, O.; Mir, M.; Knoll, W. *J. Phys. Chem. B* **2007**, *111*, 13499.
- 69) Reviakine, I.; Brisson, A. *Langmuir* **2001**, *17*, 8293.
- 70) Kim, K.; Yang, H.; Jon, S.; Kim, E.; Kwak, J. *J. Am. Chem. Soc.* **2004**, *126*, 15368.
- 71) Reznik, G. O.; Vajda, S.; Cantor, C. R.; Sano, T. *Bioconjugate Chem.* **2001**, *12*, 1000.

- 72) Huang, N.-P.; Vörös, J.; De Paul, S. M.; Textor, M.; Spencer, N. D. *Langmuir* **2002**, *18*, 220.
- 73) Kim, N. H.; Baek, T. J.; Park, H. G.; Seong, G. H. *Anal. Sci.* **2007**, *23*, 177.
- 74) Yang, Z. P.; Belu, A. M.; Liebmann-Vinson, A.; Sugg, H.; Chilkoti, A. *Langmuir* **2000**, *16*, 7482.
- 75) Hyun, J.; Zhu, Y.; Liebmann-Vinson, A.; Beebe, T. P.; Chilkoti, A. *Langmuir* **2001**, *17*, 6358.
- 76) Höök, F.; Ray, A.; Norden, B.; Kasemo, B. *Langmuir* **2001**, *17*, 8305.
- 77) Gronewold, T. M. A.; Baumgarten, A.; Quandt, E.; Famulok, M. *Anal. Chem.* **2006**, *78*, 4865.
- 78) Curie, J.; Curie, P. *Comput. Rend. Acad. Sci. Paris* **1880**, *91*, 294.
- 79) Sauerbrey, G. *Z. Phys* **1959**, *155*, 206.
- 80) Dixon, M. C. *J Biomol Tech.* **2008**, *19*(3), 151.
- 81) Baltus, R. E.; Carmon, K. S.; Luck, L. A. *Langmuir* **2007**, *23*, 3880.
- 82) Vashist, S. K.; Vashist, P. *Journal of Sensors* 2011, 2011, Article ID 571405.
- 83) King, W.H. *Anal. Chem.* **1964**, *36*, 1735.
- 84) Guilbault, G. G. *Anal. Chem.* **1983**, *55*, 1682.
- 85) O'Sullivan, C. K.; Guilbault, G. G. *Biosens. Bioelectron.* **1999**, *14*(8-9), 663.
- 86) Nakamura, C.; Song, S.-H.; Chang, S.-M.; Sugimoto, N.; Miyake, J. *Anal. Chim. Acta* **2002**, *469*(2), 183.
- 87) Samoylov, A. M.; Samoylova, T. I.; Pathirana, S. T.; Globa, L. P.; Vodyanoy, V. *J. J. Mol. Recognit.* **2002**, *15*, 197.

- 88) Peng, H.; Liang, C.; Zhou, A.; Zhang, Y.; Xie, Q.; Yao, S. *Anal. Chim. Acta* **2000**, 423, 221.
- 89) Yao, S.; Peng, H.; Liang, C.; Wu, Y.; Nie, L. *Anal. Sci.* **2000**, 16, 211.
- 90) Haupt, K.; Noworyta, K.; Kutner, W. *Anal. Commun.* **1999**, 36, 391.
- 91) Marx, S.; Kaushansky, N.; Gratziany, N.; Barness, I.; Liron, Z. *Biosens. Bioelectron.* **2001**, 16, 239.
- 92) Johnsson, M.; Bergstrand, N.; Edwards, K.; Stalgren, J. J. R. *Langmuir* **2001**, 17, 3902.
- 93) Cao, L.; Zhou, X. C.; Li, S. F. Y. *Analyst* **2001**, 126, 184.
- 94) Tan, Y.; Peng, H.; Liang, C.; Yao, S. *Sens. Actuators B* **2001**, 73, 179.
- 95) Attili, B. S.; Suleiman, A. A. *Microchem. J.* **1996**, 54, 174.
- 96) Halámek, J.; Makower, A.; Skládal, P. *Biosens. Bioelectron.* **2002**, 17, 1045.
- 97) Zhu, W.; Wei, W.; Nie, L.; Yao, S. *Anal. Chim. Acta* **1993**, 282, 535.
- 98) Chance, J. J.; Purdy, W. C. *Anal. Lett.* **1999**, 32, 1751.
- 99) O'Sullivan, C. K.; Guilbault, G. G. *Biosens. Bioelectron.* **1999**, 14, 663.
- 100) Schakenraad, J. M.; Arends, J.; Busscher, H. J.; Dijk, F.; van Wachem, P. B.; Wildevuur, C. R. H. *Biomaterials* **1989**, 10, 43.
- 101) Van Kooten, T. G.; Schakenraad, J. M.; van der Mei, H. C.; Busscher, H. J. *Biomaterials* **1992**, 13, 897.
- 102) Ruady, T. G.; Moorlag, H. E.; Schakenraad, J. M.; Van der Mei, H. C.; Busscher, H. J. *J. Colloid Interface Sci.* **1997**, 188, 209.
- 103) Vasina, E. N.; Déjardin, P. *Biomacromolecules*, **2003**, 4, 304.

104) Fredriksson, C.; Kihlman, S.; Rodahl, M.; Kasemo, B. *J. Mater. Sci. Mater. Med.* **1998**, *9*, 785.

105) Marx, K. A.; Zhou, T.; Schulze, H.; Montrone, A.; Braunschweig, S. J. *Biosens. Bioelectron.* **2001**, *16*, 773.

## **Chapter 2: Experimental**

### **2.1. Materials**

All reagents were purchased from Sigma-Aldrich and VWR companies and were used without further purification. All solvents were of analytical grade and were properly distilled and collected immediately prior to use, if needed. Milli-Q quality water (>18 M $\Omega$  resistance) was used for all the measurements. A stock solution of all the proteins (1mg/mL) in phosphate buffer saline solution (PBS) of pH 7.4 was prepared and stored at -20°C.

### **2.2. Characterization**

$^1\text{H}$  NMR spectra were recorded on a JEOL ECS-500 for  $^{13}\text{C}$  NMR and JEOL ECX- 400 for  $^1\text{H}$  NMR. UV-vis measurements were taken on an Agilent technologies 8453 spectrometer.

### **2.3. Film Fabrication**

Thin films were fabricated onto Surface Plasmon Resonance (SPR) – grade gold (Au) substrates from biotinylated carbazole using an electrochemical polymerization technique in both *ex situ* and *in situ* set-up with respect to the SPR. The Au film deposition onto the BK7 glass substrates was performed using a thermal evaporator

(Edwards E305) with a 2-5 nm thick chromium adhesion layer at a deposition rate of 0.2 Å sec<sup>-1</sup> and 50 nm Au at a deposition rate of 1.0 Å sec<sup>-1</sup> to 1.2 Å sec<sup>-1</sup> operating under high vacuum (10<sup>-6</sup> bar). The evaporated Au substrates were subjected to oxygen plasma cleaning (Plasmod, March Instruments) for 120 seconds. These substrates were used as working electrodes for the electrochemistry experiments.

All electropolymerizations were performed using the Autolab PGSTAT 12 potentiostat (Metrohm) coupled with an SPR instrument (Autolab ESPRIT from Eco Chemie). The potentiostat instrument is controlled by a GPES version 4.9 software which was provided by MetrOhm and Eco-Chemie. The electropolymerization was performed using cyclic voltammetry (CV) in a three-electrode cell containing different concentrations of the OEGylated carbazole dendron monomers and 0.1 M tetrabutylammonium hexafluorophosphate (TBHP) as supporting electrolyte in acetonitrile by sweeping the voltage from 0 V to 1.1 V for 20 cycles at a scan rate of 50 mV/s against a Ag/AgCl non-aqueous reference electrode and Pt counter-electrode. For the *ex situ* set-up (not coupled to SPR instrument), the electropolymerization was performed using the evaporated gold substrate inserted onto a fabricated electrochemical cell (Teflon made) with a diameter of 1.0 cm and volume of 0.785 cm<sup>3</sup>.

## **2.4. Atomic Force Microscopy (AFM)**

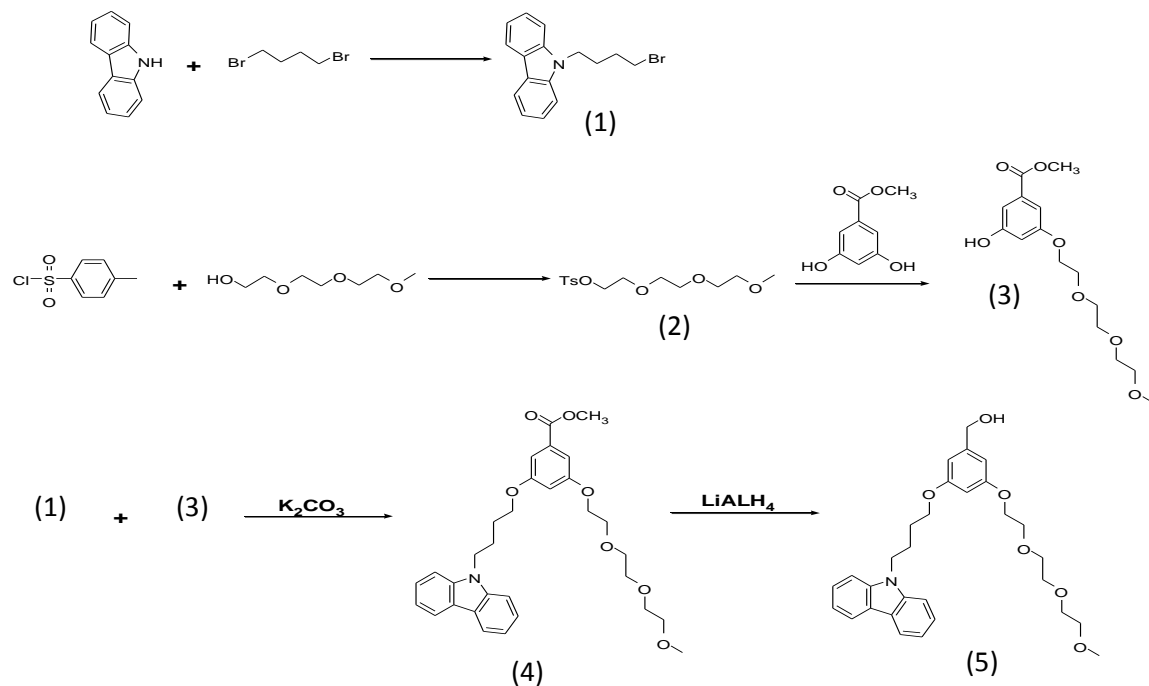
The AFM measurements were carried out using a piezoscanner capable of scanning an area of  $\sim 5 \times 5 \mu\text{m}$  at room temperature. Commercially available tapping mode tips (TAP300, Silicon AFM Probes, Ted Pella, Inc.) were used on cantilevers with a resonance frequency in the range 290-410 kHz. All images (AFM topography, Tapping mode) were filtered and analyzed by using SPIP software (Scanning Probe Image Processor, Image Metrology A/S). All data in the dimensions of surface aggregates were collected and averaged by at least 20 measurements from line profilometry of the AFM images. Lateral size and height of the aggregate were determined after calibration of AFM tips using a defined patterned surface (MIKRO MASCH, size: 100 nm).

## **2.5. Quartz Crystal Microbalance**

The QCM apparatus, probe, and crystals are available from MAXTEK Inc. The data acquisition was done using a RQCM (Research Quartz Crystal Microbalance, MAXTEK, Inc.) system equipped with an in-built phase lock oscillator, and the RQCM Data-Log Software. This was coupled with the Amel potentiostat to generate EC-QCM results. A 5 MHz AT-cut Au-coated quartz crystal with an effective area of  $1.327 \text{ cm}^2$  was used as a working electrode. Platinum as a counter electrode and Ag/AgCl as a reference were used to measure in-situ polymer adsorption changes during cyclic voltammetry.



## 2.6. Synthesis



**Scheme 2.1** Synthesis of PEGylated carbazole.

**2.6.1. Synthesis of 9-(4-Bromobutyl)-9H-carbazole (1).** To a 1000 mL round-bottom flask were added carbazole (20.64 g, 0.12 mol), 1,4-dibromobutane (131.2 mL, 1.09 mol), 50 % NaOH (200 mL), tetra-*n*-butyl ammonium bromide (4.0 g, 12 mmol), and 200 mL of toluene. The mixture was refluxed at 45°C for 3 hours. It was then stirred overnight at room temperature. The completion of the reaction was monitored with thin layer chromatography (TLC) using (2:1) hexanes/dichloromethane as the developing solvent. The clear, yellow organic layer was then washed with 100-mL portions H<sub>2</sub>O followed by 100 mL brine solution. After filtration, the solvent was evaporated and the excess of tetra-*n*-butyl ammonium bromide was removed by vacuum distillation. The

solid was dissolved in small amount of dichloromethane and was recrystallized from ethanol. A white colored solid was obtained in 83% yield.  $^1\text{H}$  NMR ( $\text{CDCl}_3$ , 400 MHz)  $\delta$  1.85-1.92 (m, 2H), 1.99-2.07 (m, 2H), 3.34 (t,  $J = 6.4$  Hz, 2H), 4.31 (t,  $J = 6.88$  2H) 7.21-7.27 (m, 2H), 7.37 (d,  $J = 8.24$ , 2H), 7.42-7.47 (m, 2H), 8.09 (d,  $J = 7.8$ , 2H);  $^{13}\text{C}$  NMR ( $\text{CDCl}_3$ , 125 MHz)  $\delta$  27.77, 30.35, 33.36, 108.70, 119.10, 120.57, 123.01, 125.87, 140.40.

**2.6.2. Synthesis of Toluene-4-sulfonic acid-2-[2-(2-methoxyethoxy)-ethoxy]ethyl ester (2).** To a 500 mL round bottom flask were added triethylene glycol monomethyl ether (10 g, 60 mmol), triethylamine (6 ml, 43 mmol), and acetonitrile (5 ml). A solution of para-toluenesulfonyl chloride (14.4 g, 73 mmol) in acetonitrile was then added dropwise. After stirring overnight, the white solid was filtered off and the resulting solution was extracted three times with dichloromethane. The combined dichloromethane extracts were washed with water and dried with sodium sulfate. The solvent was evaporated and the resulting mixture was subjected to column chromatography using (1:1) ethylacetate/hexanes as eluent. The product was obtained as yellow colored oil in 58 % yield.  $^1\text{H}$  NMR ( $\text{CDCl}_3$ , 400 MHz)  $\delta$  2.35-2.37 (m, 3H), 3.26-3.29 (m, 3H), 3.41-3.45 (m, 2H), 3.48-3.52 (m, 6H), 3.57-3.60 (m, 2H), 4.04-4.07 (m, 2H), 7.25-7.28 (m, 2H), 7.68-7.73 (m, 2H);  $^{13}\text{C}$  NMR ( $\text{CDCl}_3$ , 125 MHz)  $\delta$  21.45, 58.79, 68.44, 69.20, 70.32, 70.48, 71.69, 127.77, 129.73, 132.75, 144.72.

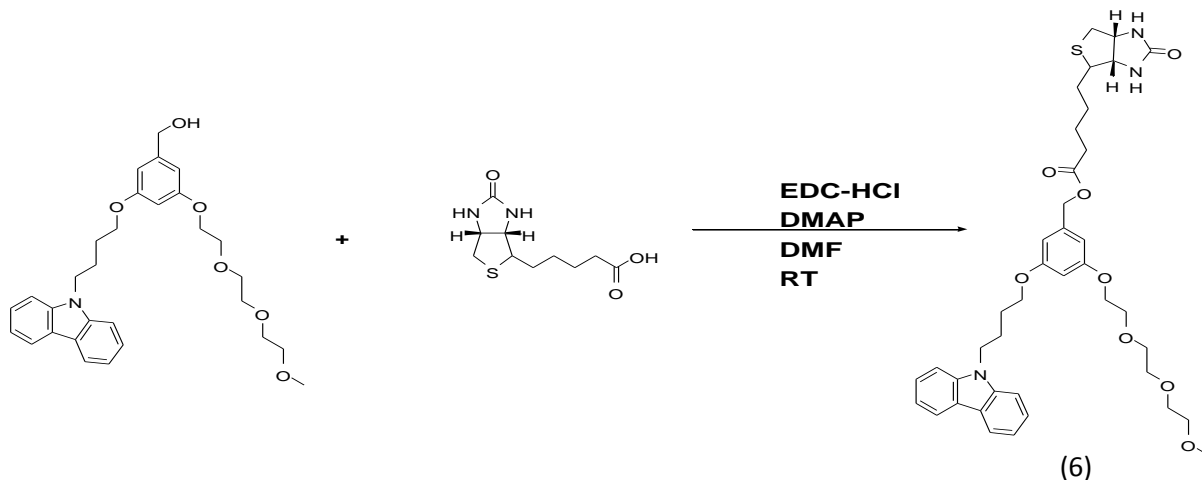
**2.6.3. Synthesis of 3-Hydroxy-5-{2-[2-(2-methoxyethoxy)ethoxy]ethoxy}benzoic acid methyl ester. (3).** To a 250 mL round bottom flask, were added methyl-3,5-dihydroxy benzoate (5.27 g, 2 mol), compound **2** (5 g, 1 mol), potassium carbonate (2.6 g, 1.2 mol), and 18-crown-6 ether (0.9 g, 0.23 mol). The mixture was dissolved in acetone and refluxed overnight with constant stirring. The solvent was evaporated and the resulting mixture was extracted three times with dichloromethane. The combined dichloromethane extracts were washed with water, brine, and was dried with sodium sulfate. The resulting mixture was subjected to column chromatography using (1:1) ethyl acetate/hexanes as eluent. The product was obtained as light brown colored oil in 34 % yield. <sup>1</sup>H NMR (CDCl<sub>3</sub>, 400 MHz) δ 3.37 (s, 3H), 3.56-3.59 (m, 2H), 3.64-3.69 (m, 4H), 3.81-3.83 (m, 2H), 3.87 (s, 3H), 4.09-4.11(m, 2H), 6.66 (t, *J* = 2.32, 2H), 7.05-7.07 (m, 1H), 7.11-7.12 (m, 1H). <sup>13</sup>C NMR (CDCl<sub>3</sub>, 125 MHz) δ 52.39, 59.19, 67.85, 69.73, 70.71, 70.78, 70.98, 72.05, 107.02, 108.14, 131.99, 159.87, 166.94.

**2.6.4. Synthesis of (3-(4-Carbazol-9-yl-butoxy)-5-{2-[2-(2-methoxyethoxy)-ethoxy]-ethoxy}-benzoic acid methyl ester (4).** To a 250 mL round bottom flask were added compound **3** (0.867 g, 1 mol), compound **1** (1.66 g, 2 mol), potassium carbonate (1.14 g, 3 mol), 18-crown-6 ether (0.07 g, 0.1 mol). The mixture was dissolved in acetone and refluxed for two days with constant stirring. The solvent was evaporated and the resulting mixture was extracted three times with dichloromethane. The combined dichloromethane extracts were washed with water, brine, and dried with sodium sulfate. After filtration, the solvent was evaporated and the resulting mixture was subjected to column chromatography using (1:1) ethyl acetate/hexanes as the eluent system. Light brown

liquid was obtained in 75 % yield.  $^1\text{H}$  NMR ( $\text{CDCl}_3$ , 400 MHz)  $\delta$  1.82-1.86 (m, 2H), 2.06-2.10 (m, 2H), 3.36 (s, 3H), 3.52-3.55 (m, 2H), 3.63-3.68 (m, 4H), 3.72-3.74 (m, 2H), 3.84 (t,  $J = 4.6$ , 2H), 3.95 (t,  $J = 6.4$ , 2H), 4.12 (t,  $J = 5.04$ , 2H), 4.40 (t,  $J = 6.88$ , 2H), 6.62 (t,  $J = 2.32$ , 1H), 7.13-7.14 (m, 1H), 7.16-7.17 (m, 1H), 7.21-7.25 (m, 2H), 7.41-7.48 (m, 4H), 8.10 (d,  $J = 7.8$ , 2H).  $^{13}\text{C}$  NMR ( $\text{CDCl}_3$ , 125 MHz)  $\delta$  25.95, 27.03, 42.80, 52.38, 59.18, 67.83, 67.89, 69.72, 70.70, 70.79, 70.96, 72.05, 106.79, 107.84, 108.14, 108.76, 118.98, 120.52, 122.98, 125.98, 132.03, 140.46, 159.91, 159.96, 166.92.

**2.6.5. Synthesis of (3-(4-Carbazol-9-yl-butoxy)-5-{2-[2-(2-methoxyethoxy)-ethoxy]-ethoxy}-phenyl)-methanol (5).** Compound **4** (4.73 g, 1 mol) was dissolved in minimum amount of dry THF. It was then transferred to a 250 mL three-necked flask previously flowed with nitrogen. The flask was put in an ice bath. Lithium aluminium hydride (0.6 g, 1.77 mol) was then added to the flask and was stirred for 10 mins. The ester solution was then added dropwise and the resulting solution was stirred overnight. The reaction mixture was quenched with water under cooling. It was then acidified with concentrated hydrochloric acid. The resulting mixture was extracted three times with dichloromethane. The combined dichloromethane extracts were washed with water and the organic layer was dried with sodium sulfate. After filtration, the solvent was evaporated. A white solid was obtained in 82 % yield.  $^1\text{H}$  NMR ( $\text{CDCl}_3$ , 400 MHz)  $\delta$  1.81-1.85 (m, 2H), 2.05-2.09 (m, 2H), 3.36 (s, 3H), 3.52-3.54 (m, 2H), 3.62-3.68 (m, 4H), 3.71-3.73 (m, 2H), 3.92 (t,  $J = 5.96$ , 2H), 4.09 (t,  $J = 5.04$ , 2H), 4.39 (t,  $J = 7.32$ , 2H), 4.59 (s, 2H), 6.35 (t,  $J = 2.28$ , 1H), 6.46 (s, 1H), 6.52 (s, 1H), 7.21-7.25 (m, 3H), 7.41-7.48 (m, 4H), 8.10 (d,  $J = 7.8$ , 2H).  $^{13}\text{C}$  NMR ( $\text{CDCl}_3$ , 125 MHz)  $\delta$  26.02, 27.12, 42.85, 59.19, 65.35, 67.60, 67.65,

69.85, 70.68, 70.80, 70.93, 72.05, 100.80, 105.35, 105.48, 108.81, 118.99, 120.54, 122.99, 125.82, 140.50, 143.59, 160.25, 160.30.



**Scheme 2.2** Synthesis of biotinylated carbazole.

**2.6.6. Synthesis of 5-(2-Oxo-hexahydro-thieno[3,4-d]imidazole-4-yl)-pentanoic acid 3-(4-carbazol-9-yl-butoxy)-5-{2-[2-(2-methoxyethoxy)-ethoxy]-ethoxy}-benzyl ester (6).** In a 100 mL round bottom flask, compound **5** (500 mg, 1 mol), biotin (292 mg, 1 mol), and 4-dimethylaminopyridine (146 mg, 1 mol) were dissolved in minimum amount of dry DMF. Nitrogen gas was passed through the flask and the reaction mixture was sonicated for 5 mins. The flask was kept in an ice bath and nitrogen gas was continuously flowed through the flask. 185.20 mg of 1-ethyl-3-(3-dimethylaminopropyl)carbodiimide (1 mol) was dissolved in minimum amount of dry THF, and added to the above mixture dropwise while the ice-cold flask was under nitrogen. The reaction mixture was stirred overnight at room temperature. DMF was removed by vacuum distillation and the

resulting mixture was extracted three times with dichloromethane. The combined dichloromethane extracts were washed with water and dried with sodium sulfate. The resulting residue was purified by using glass silica gel TLC plates using 3 % methanol in dichloromethane as the eluent. The product was obtained as brown-colored oil in 8 % yield.  $^1\text{H}$  NMR (DMSO, 400 MHz)  $\delta$  1.18-1.56 (m, 6H), 1.65-1.72 (m, 2H), 1.84-1.91 (m, 2H), 2.31 (t,  $J = 7.2$ , 2H), 2.46-2.53 (m, 2H), 2.99-3.01 (m, 1H), 3.17 (s, 1H), 3.26-3.38 (m, 12H), 3.44-3.52 (m, 6H), 3.65-3.67 (m, 2H), 3.90 (t,  $J = 6.4$ , 2H), 3.98-4.00 (m, 2H), 4.05-4.06 (m, 1H), 4.21-4.25 (m, 1H), 4.43 (t,  $J = 7.2$ , 2H), 4.93 (s, 2H), 6.33-6.44 (m, 5H), 7.14-7.17 (m, 2H), 7.39-7.43 (m, 2H), 7.59 (d,  $J = 8$ , 2H), 8.11 (d,  $J = 7.2$ , 2H).  $^{13}\text{C}$  NMR (DMSO, 125 MHz)  $\delta$  24.75, 25.50, 26.52, 28.23, 33.50, 42.11, 55.58, 58.25, 59.40, 61.23, 65.37, 67.39, 67.48, 69.11, 69.82, 70.02, 70.14, 71.48, 100.63, 106.32, 106.50, 109.47, 118.90, 120.49, 122.27, 125.90, 138.71, 140.18, 159.86, 159.99, 162.97, 172.93.

### Chapter 3: Results and Discussion

The study on electrochemical microdevices has been gaining interest in the past decade because of their potential application in clinical analysis and environmental control.<sup>1</sup> Among the conventional methods of microtransducer functionalization, the immobilization of biomolecules on electropolymerized films is attracting attention. Previous studies in our group have shown that electrochemical deposition could precisely generate a polymer film on conductive microsurfaces of complex geometry.<sup>2-10</sup> During the electropolymerization, the electroactive functional groups are connected providing a networked structure on the surface. In addition, the generated polymer films exhibited good robustness in both aqueous and organic media.

The main challenge in surface functionalization for affinity-based methods is to immobilize one of the interacting compounds on the surface in such a way that nonspecific interactions of the protein with the surface are minimized.<sup>11-13</sup> Keeping in mind the possibility of both specific and nonspecific adsorption of streptavidin on surfaces, this study is designed to incorporate poly(ethylene glycol) as a protein resistant functional moiety and biotin for the formation of biotin-streptavidin bridge for protein immobilization.

Overall, the study is aimed at providing a new platform for the immobilization of streptavidin via electrochemical grafting. The ability to fine-tune the formation of polymer film with electrochemically controlled thickness will enable the engineering of

new molecular templates for biosensor applications. The present design incorporates carbazole for electrochemical grafting on the surface, poly(ethylene glycol) to prevent nonspecific adsorption and biotin for the specific binding of streptavidin (Figure 3.1).

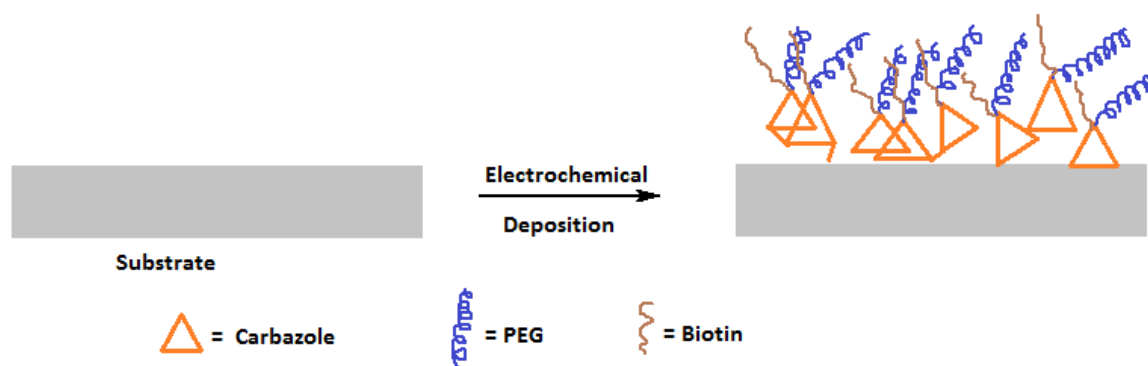
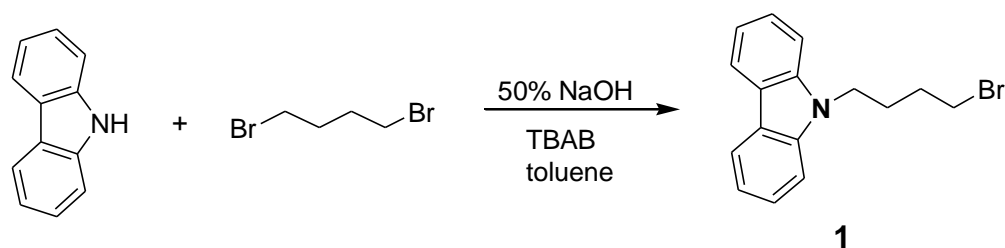


**Figure 3.1** Molecular design of the study.

### 3.1. Synthesis

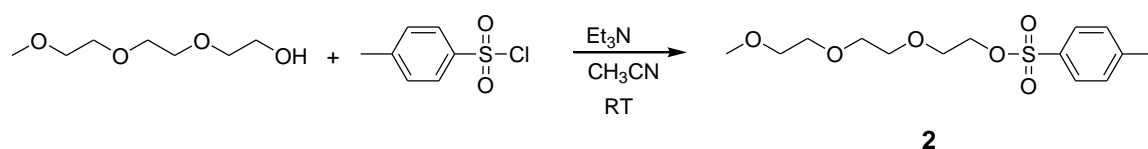


**Scheme 3.1** Synthesis of 9-(4-Bromobutyl)-9H-carbazole

Compound **1** was synthesized by reaction of carbazole and 1,4-dibromobutane as discussed in the previous chapter (Scheme 3.1). Tetra-*n*-butylammonium bromide (TBAB) was used as a phase transfer catalyst to facilitate the reaction between organic

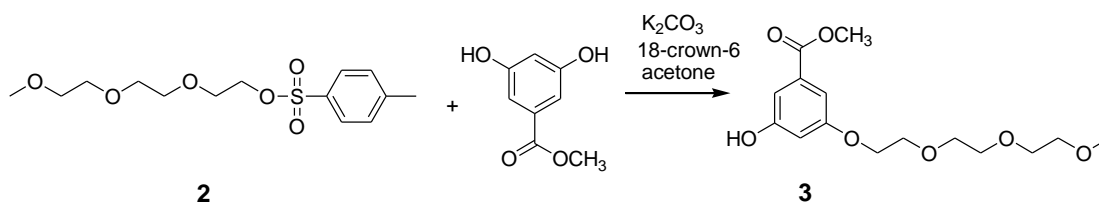


and aqueous reagents present in the reaction mixture. The purity of the product was confirmed by  $^1\text{H}$  NMR. Compound **2** was obtained by an  $\text{S}_{\text{N}}2$  reaction of triethylene glycol monomethyl ether with para-toluenesulfonyl chloride in presence of triethyl amine at room temperature in acetonitrile solvent (Scheme 3.2). Thus the -OH group of triethylene glycol monomethyl ether is converted to a tosyl group which is a good leaving group and facilitates ether formation in the next step.



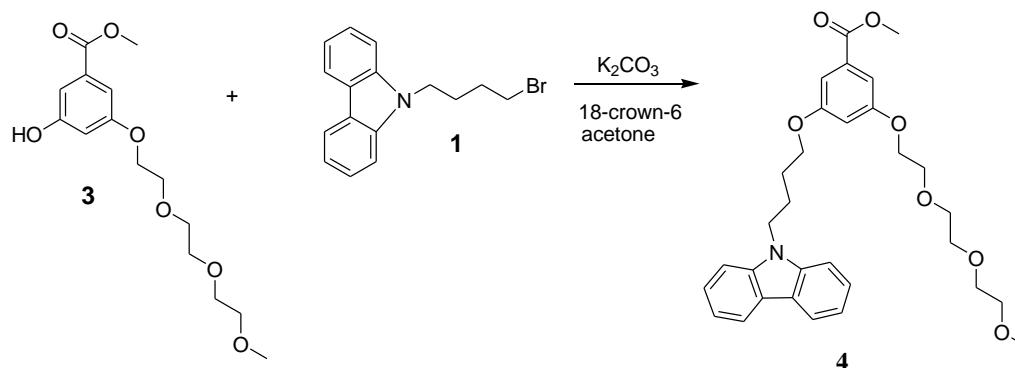
**Scheme 3.2** Synthesis of Toluene-4-sulfonic acid-2-[2-(2-methoxyethoxy)-ethoxy]ethyl ester

Compound **2** was further used for selective functionalization of one of the OH groups of methyl-3,5-dihydroxybenzoate (Scheme 3.3). Thus compound **3** was obtained by an  $\text{S}_{\text{N}}2$  reaction and the use of the phase transfer catalyst 18-crown-6, to facilitate the solubility of the inorganic base  $\text{K}_2\text{CO}_3$  in organic phase, at relatively mild reaction conditions.



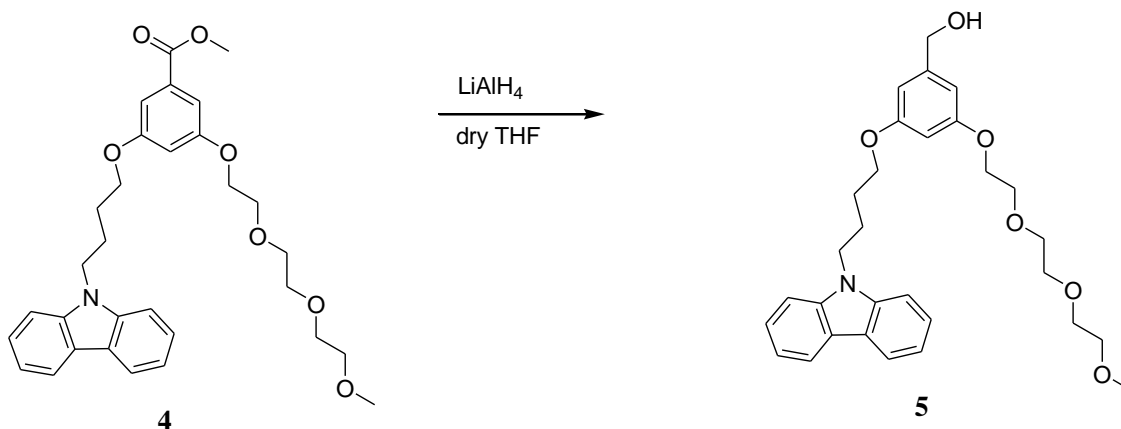
**Scheme 3.3** Synthesis of 3-Hydroxy-5-{2-[2-(2-methoxyethoxy)ethoxy]ethoxy} benzoic acid methyl ester.

Compound **3** was then treated with compound **1** in the presence of the inorganic base, potassium carbonate and the phase transfer catalyst 18-crown-6 (Scheme 3.4) to obtain compound **4**. The identity and purity of **4** was confirmed by  $^1\text{H}$  NMR. The reaction takes place via an  $\text{S}_{\text{N}}2$  mechanism. The ester group in compound **4** was reduced by lithium aluminium hydride (LAH) to yield the corresponding alcohol **5** (Scheme 3.5). The disappearance of a singlet peak at  $\delta$  3.88 ppm and the appearance of a new singlet peak at  $\delta$  4.59 ppm in the  $^1\text{H}$  NMR confirms the successful conversion of an ester to a benzylic alcohol. This is further confirmed from the  $^{13}\text{C}$  NMR which shows 25 and 24 signals for ester and alcohol respectively. The reaction proceeds through the



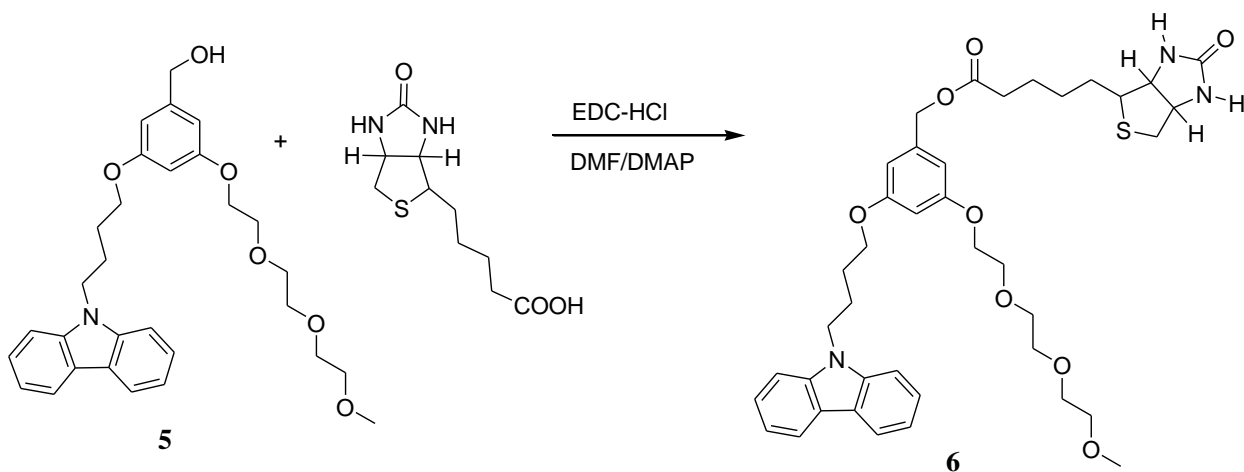
**Scheme 3.4** Synthesis of (3-(4-Carbazol-9-yl-butoxy)-5-{2-[2-(2-methoxyethoxy)-ethoxy]-ethoxy}-benzoic acid methyl ester

formation of an aldehydic intermediate which is further reduced to the corresponding benzylic alcohol **5**.



**Scheme 3.5** Synthesis of (3-(4-Carbazol-9-yl-butoxy)-5-{2-[2-(2-methoxyethoxy)-ethoxy]-ethoxy}-phenyl)-methanol

The  $-\text{OH}$  group in compound **5** reacts with the carboxylic group of biotin to give the biotinylated compound **6** (Scheme 3.6). The reaction proceeds through EDC-DMAP coupling chemistry to form an ester bond in **6**. The product was obtained in pure form and characterized by  $^1\text{H}$  NMR and  $^{13}\text{C}$  NMR. In  $^1\text{H}$  NMR, the benzylic proton in **6** appears at  $\delta$  4.95 ppm. The shift of the benzylic proton peak to a higher chemical shift value as compared to the alcohol benzylic proton peak which appears at  $\delta$  4.59 ppm confirms formation of an ester bond. The singlet peaks at  $\delta$  6.52 and 6.46 ppm are attributed to protons attached to the nitrogen atoms in the biotin moiety.



**Scheme 3.6** Synthesis of 5-(2-Oxo-hexahydro-thieno[3,4-d]imidazole-4-yl)-pentanoic acid 3-(4-carbazol-9-yl-butoxy)-5-{2-[2-(2-methoxyethoxy)-ethoxy]-ethoxy}-benzyl ester

### 3.2. Film Fabrication: Electrochemical Deposition

Previous studies showed that carbazole is easily polymerized by cyclic voltammetry at low potential, resulting in polycarbazole linkages.<sup>2-10</sup> Several studies on the electrochemical oxidation of carbazole have been reported.<sup>14-20</sup> Ambrose *et al.* investigated the anodic oxidation of carbazole and its N-substituted derivatives.<sup>14-15</sup> They suggested that the formation of the dicarbazyl dication at the 3- and 3'- positions is the predominant pathway during anodic oxidation (Figure 2). On the other hand, several groups reported the electrodeposition of longer polycarbazole film under suitable conditions.<sup>14-20</sup> The target biotinylated compound was designed to have the carbazole to offer electropolymerizability.

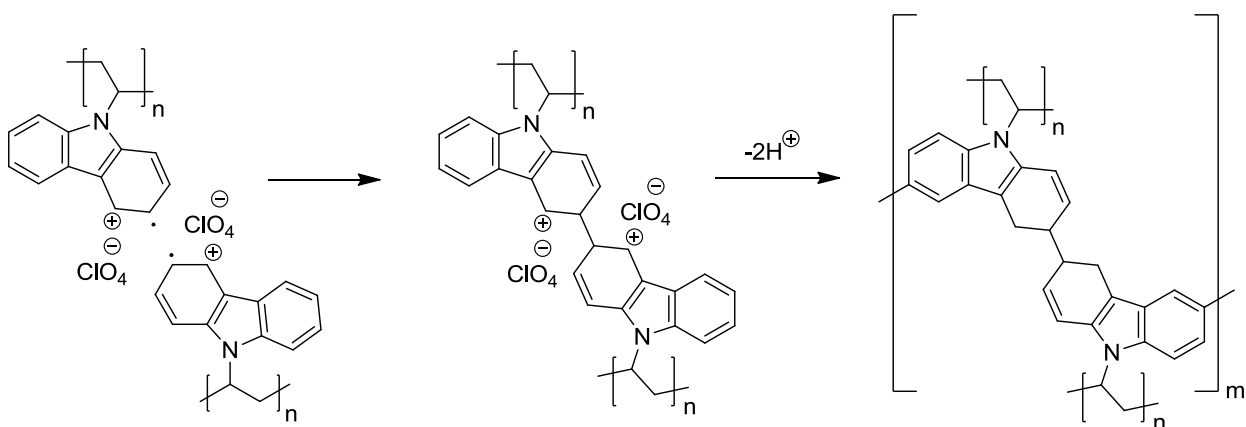


**Figure 3.2** Cross-linking of carbazole.

To explore the electrochemical grafting of the synthesized biotinylated carbazoles, various concentrations of compound **6** were deposited on Au substrate by cyclic voltammetry (CV). The CV deposition of **6** dissolved in HPLC grade acetonitrile (0.01 % max. water) was performed in a three-electrode cell containing 0.1 M tetrabutylammonium hexafluorophosphate (TBAH) as the supporting electrolyte. The electropolymerization was performed in each case by sweeping the voltage at a scan rate of 50 mV/s from 0 to 1.3 V against Ag/AgCl as a reference electrode and Pt as a counter electrode. Electrodeposition of the films was done in 20 cycles. Figure 3.3 shows the CV traces of 200  $\mu$ M, 500  $\mu$ M, and 1 mM solution of biotinylated carbazoles.

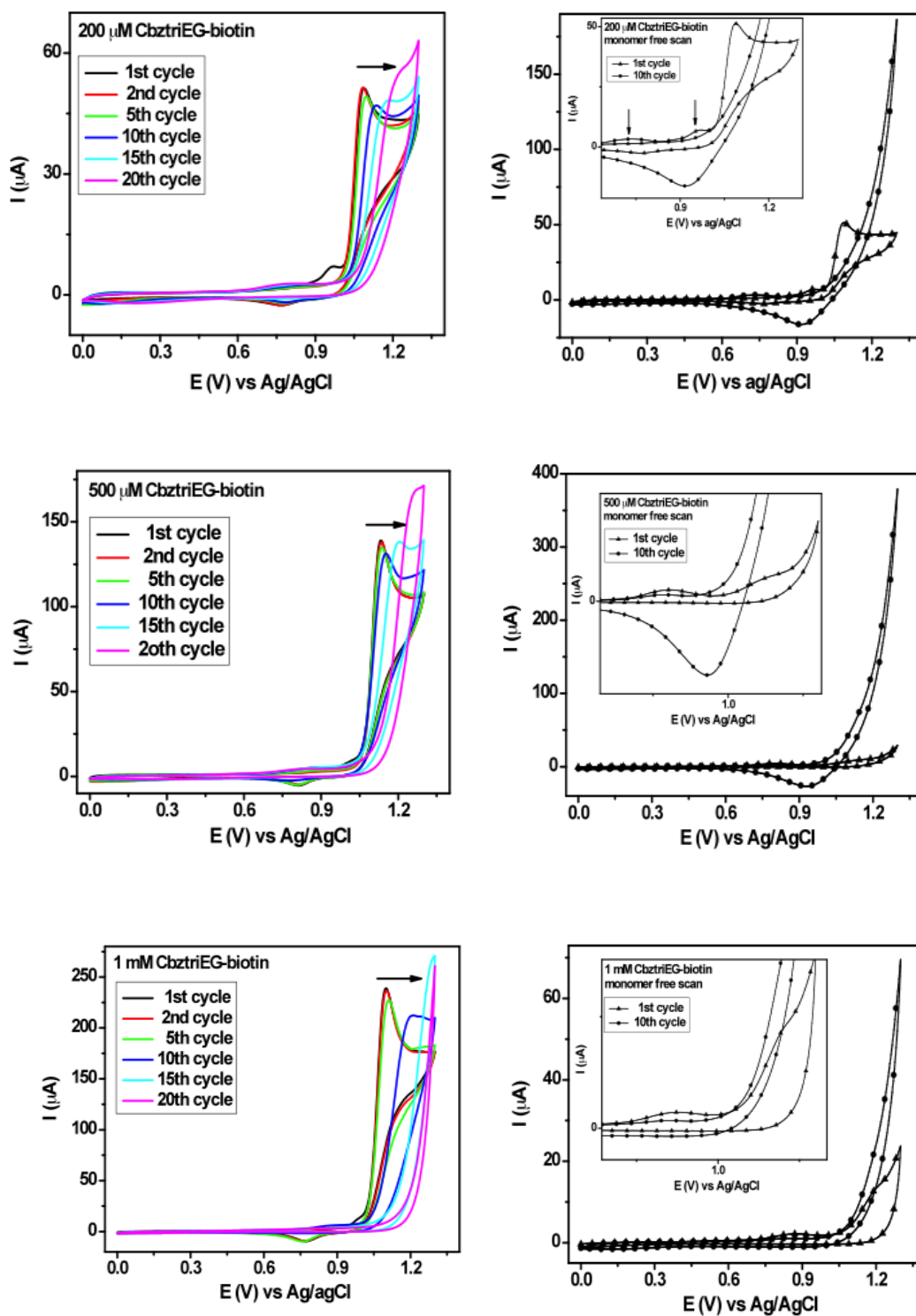


**Figure 3.3** CV traces of (a) 200  $\mu$ M, (b) 500  $\mu$ M, and (c) 1 mM biotinylated compound 6 in acetonitrile; and monomer-free scan of (d) 200  $\mu$ M, (e) 500  $\mu$ M, and (f) 1 mM solutions.

From the cyclic voltammogram, the strong peaks at 0.84 – 0.89 V and 1.1-1.3 V (vs Ag/AgCl) for all the concentrations are due to the oxidation of the polycarbazole. The CV diagrams give a clear evidence of the electrografting behavior of the carbazole units. This represents the generation of radical cation species that lead to coupling of carbazoles at the 3,6-position and subsequent oligomerization. In addition, the oxidation peak potential shifts gradually to slightly higher values as the number of cycles increases. This effect indicates more heterogeneous and slow electron-transfer kinetics.<sup>7</sup>

**Table 3.1.** Ellipsometric thickness of films fabricated from compound **6**.

| Concentration | Thickness<br>(Ellipsometry) (Å) |
|---------------|---------------------------------|
| 200 $\mu$ M   | 80.9 $\pm$ 6.0                  |
| 500 $\mu$ M   | 112.1 $\pm$ 3.4                 |
| 1 mM          | 128.5 $\pm$ 4.6                 |

These films were further analyzed using ellipsometry. From Table 3.1, it can be observed that deposition of higher concentration of **6** gives thicker films. This is expected since more materials are being deposited on the surface. AFM images (Figure 3.4) also show the full coverage of the films on the Au substrate in all the concentrations used.

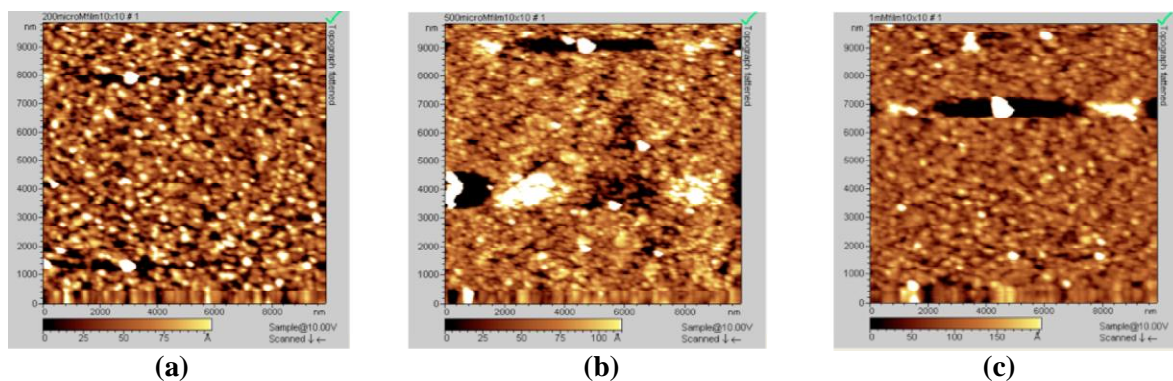


**Figure 3.4** AFM topographic images of (a) 200  $\mu\text{M}$ , (b) 500  $\mu\text{M}$ , and (c) 1 mM biotinylated compound **6** on Au substrate.

Electrochemical deposition technique has the advantage of being applicable to a large variety of substrates, including metals and alloys, semiconductors, ITO-coated glass, and carbon.<sup>5, 21</sup> A 5 mM solution of compound **6** in acetonitrile was cycled 20 times at 0-1.3 V on an indium tin oxide (ITO) substrate. The electrodeposited film was further characterized by UV-vis spectroscopy. The peak with absorption maxima at 450 nm corresponds to the  $\pi$  to  $\pi^*$  transitions attributed to the 3,3'-dicarbazyl radical cation (polaronic band or doped state) and the peak extending up to 800 nm can be assigned to the  $\pi$  to  $\pi^*$  transitions of the 3,3'-dicarbazyl dication (bipolaronic band or more highly doped state) or a complex of the dicarbazyl species and the hexafluorophosphate ions.<sup>5,14,20</sup> These peaks were not observed on a dropcast film of compound **6**. Therefore, these peaks confirm the formation of a highly conjugated nature of the materials deposited on the ITO substrates.



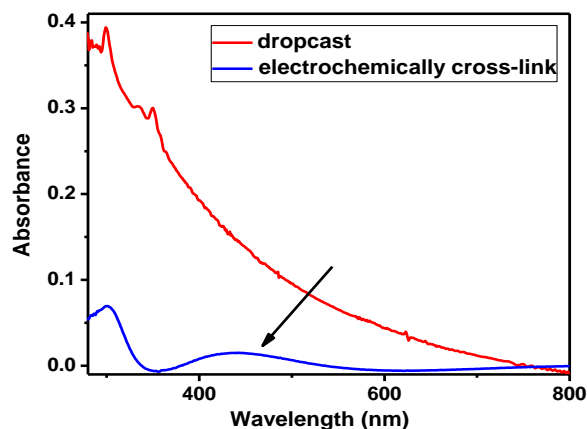


**Figure 3.5** UV-vis spectra of electrochemically grafted and dropcast of compound **6** on Indium Tin Oxide substrate.

### 3.3. Streptavidin Sensing: Electrochemical Quartz Crystal Microbalance

Binding of the biotinylated carbazole to streptavidin was evaluated by quartz crystal microbalance (QCM). Electrochemical-quartz crystal microbalance (E-QCM) was performed to monitor the change in mass and resonance resistance at the working electrode during the electrochemical deposition of the biotinylated material.<sup>22-23</sup> EC-QCM is an exceptionally versatile approach for *in situ* monitoring the gravimetric changes occurring at the electrode surfaces which relates the change in mass,  $\Delta m$ , and the change in the fundamental resonance frequency,  $\Delta F$  (Hz), of the QCM crystal by Sauerbrey equation.<sup>23</sup>

$$\Delta f = -2f_0^2 \Delta m / A(\rho_q \mu_q)^{1/2} \quad (1)$$

where  $f_0$  is the fundamental resonant frequency of the QCM (5 MHz),  $A$  is the area of the electrode ( $1.327 \text{ cm}^2$ ),  $\rho_q$  is the density of the quartz ( $2.65 \text{ g/cm}^3$ ), and  $\mu_q$  is the shear modulus of the quartz ( $2.95 \times 10^6 \text{ N/cm}^2$ ). This equation translates the changes in frequency observed during the doping and de-doping process (oxidation and reduction) to mass transport.

Figure 3.6 shows the  $\Delta F$  changes as a function of time during voltammetric cycling of 2 mM solution of compound **6** deposited from 0.1 M TBAH/acetonitrile solution at a scan rate of 20 mV/s. From Figure 3.6, a significant decrease in  $\Delta F$  changes after each CV cycle was observed indicating deposition on the QCM crystal. From the Sauerbrey equation, a decrease in the  $\Delta F$  changes indicates a corresponding deposition of a certain mass on the QCM crystal.

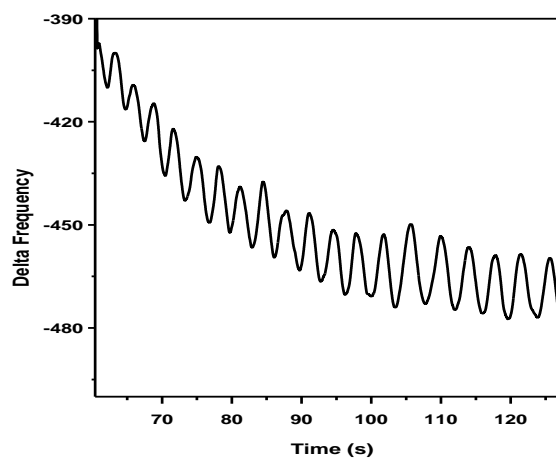


**Figure 3.6** Change in  $\Delta F$  vs. time of compound **6** on a QCM crystal.

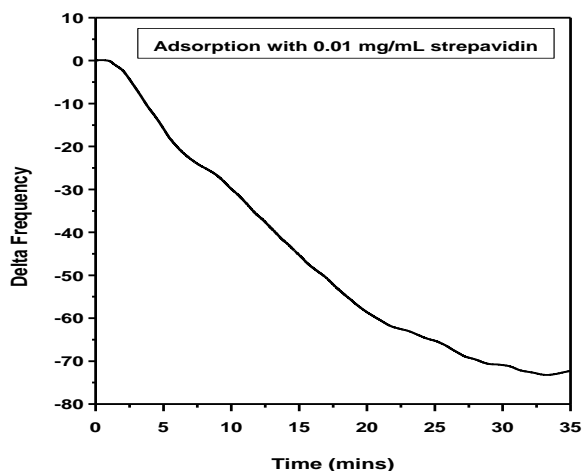


**Figure 3.7** Change in  $\Delta F$  vs. time data for the adsorption of streptavidin on a QCM crystal functionalized with biotin film.

After depositing a film of biotinylated carbazole on a QCM crystal, streptavidin binding was also monitored using QCM. From Figure 3.7, a significant change in the delta frequency indicates binding of streptavidin after 35 minutes. These data suggest that electrochemical deposition of biotin on a surface did not affect the formation of biotin-streptavidin bridge that can be used for further binding of proteins on a biosurface. Optimization of the density of the biotinylated compound on gold surface is underway.

### 3.4. References

1. Lauks, I. R. *Acc. Chem. Res.* **1998**, *31*, 317–324.
2. Ponnepati, R.; Felipe, M.J.; Muthalugu, V.; Puno, K.; Advincula, R. *ACS Appl. Mater. Interfaces* **2012**, *ASAP*.
3. Ponnepati, R.; Felipe, M.J.; Advincula, R. *Macromolecules* **2011**, *44*, 7530–7537.
4. Pernites, R.; Felipe, M.J.; Foster, E.; Advincula, R. *Adv. Mater.* **2011**, 1287–1292.
5. Felipe, M.J.; Ponnepati, R.; Dutta, P.; Advincula, R. *ACS Appl. Mater. Interfaces* **2010**, *2* (12), 3401–3405.
6. Felipe, M.J.; Dutta, P.; Pernites, R.; Ponnepati, R.; Advincula, R. *Polymer* **2012**, *2*, 427–437.
7. Taranekar, P.; Fulghum, T.; Patton, D.; Ponnepati, R.; Clyde, G.; Advincula, R. *J. Am. Chem. Soc.* **2007**, *129*, 12537–12548.
8. Jiang, G.; Ponnepati, R.; Pernites, R.; Felipe, M. J.; Advincula, R. *Macromolecules* **2010**, *43*, 10262–10274.
9. Patton, D.; Fulghum, T. M.; Taranekar, P.; Advincula, R. *Macromolecules* **2008**, *41*, 6703–6713.
10. Grande, C.; Tria, C.; Felipe, M. J.; Zuluaga, R.; Advincula, R. *Eur. Phys. J.* **2011**, *34*, 1–10.
11. Nguyen, T.; Sly, K.; Conboy, S. *Anal. Chem.* **2012**, *84*, 201–208.
12. Wolny, P.; Spatz, J.; Richter, R. *Langmuir* **2010**, *26*(2), 1029–1034.
13. Clare, T.; Clare, B.; Nichols, B.; Abbott, N.; Hamers, J. *Langmuir* **2005**, *21*, 6344–6355.

14. Ambrose, J.F.; Nelson, R.F. R. J. *Electrochem. Soc.* **1968**, *115*, 1159–1164.
15. Ambrose, J.F.; Carpenter, L.L.; Nelson, R.F. R. J. *Electrochem. Soc.* **1975**, *122*, 876–894.
16. Mengoli, G.; Musiani, M.M.; Schreck, B. J. *Electroanal. Chem.* **1988**, *246*, 73–76.
17. Macit, H.; Sen, S.; Sacak, M. J. *App. Polym. Sci.* **2005**, *96*, 894–898.
18. Inzelt, G. J. *Solid State Electrochem.* **2003**, *7*, 503–510.
19. Abe, S.Y.; Ugalde, L.; del Valle, M.A.; Tregouet, Y.; Bernede, J.C. J. *Braz. Chem. Soc.* **2007**, *18*, 601–606.
20. Kaewtong, C.; Jiang, G.; Felipe, M.J.; Pulpoka, B.; Advincula, R. *ACS Nano* **2008**, 1533–1542.
21. Gabriel, S.; Dubrue, P.; Schacht, E.; Jonas, A.; Gilbert, B.; Jerome, R.; Jerome, C. *Angew. Chem. Int. Ed.* **2005**, *44*, 5505–5509.
22. Baba, A.; Tian, S.; Stefani, F.; Xia, C.; Wang, Z.; Advincula, R.; Johannsmann, D.; Knoll, W. J. *Electroanal. Chem.*, **2004**, *562*, 95.
23. Sauerbrey, G.Z. *Phys.*, **1959**, *155*, 206.

## Chapter 4: Conclusion and Future Work

### 4.1. Conclusion

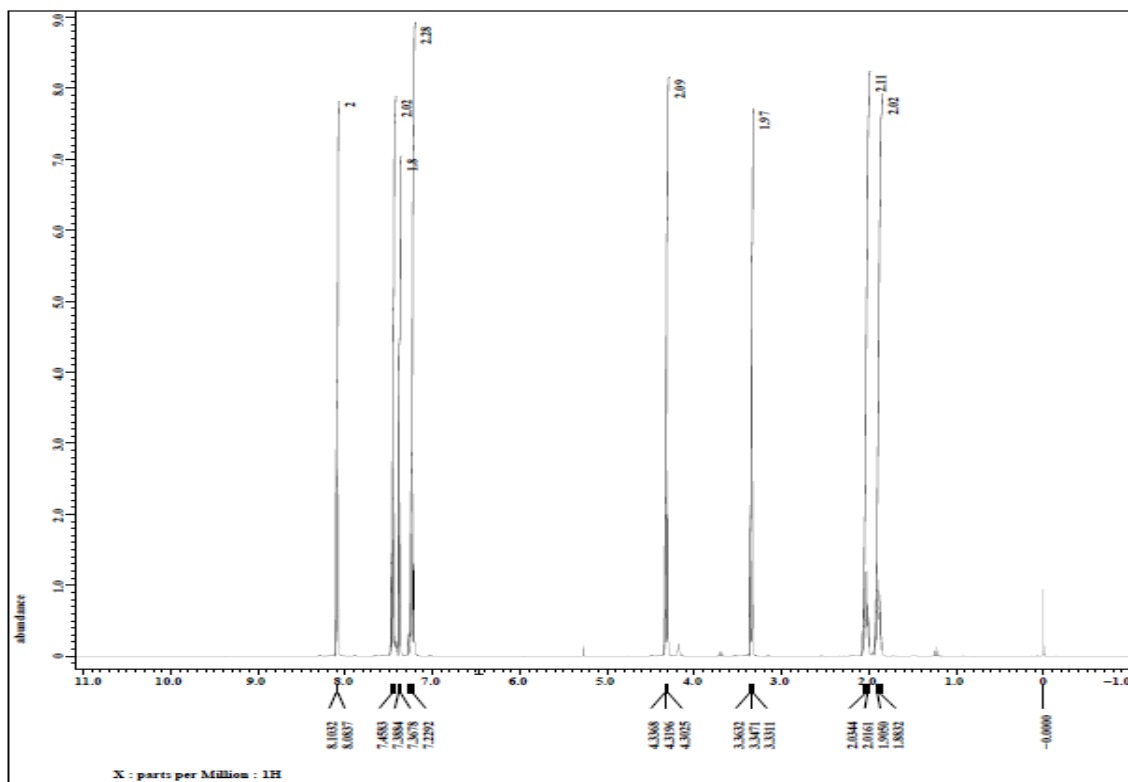
This thesis demonstrates an efficient and versatile method for the immobilization of streptavidin via electrochemical grafting. The synthesis of PEGylated carbazoles was achieved through a series of  $\text{SN}_2$  reactions which was further biotinylated through EDC-DMAP coupling reaction. The molecular design incorporates carbazole for electrochemical grafting on the surface, poly(ethylene glycol) to prevent nonspecific adsorption and biotin for the specific binding of streptavidin. Thin films of biotinylated carbazole dendrons were fabricated on QCM quartz crystal by electrochemical deposition. The electrografting behavior of carbazole was confirmed from cyclic voltammetry. In EC-QCM, the decrease in delta frequency with time confirmed the formation of a polycarbazole film on the QCM crystal. The morphologies of these films were studied by AFM which showed full coverage of the compound on the surface. These electropolymerized films were further tested for the sensing of streptavidin using QCM. A significant change in the delta frequency indicated binding of streptavidin after 35 minutes. Thus the deposition of biotin on a surface did not affect the formation of biotin-streptavidin bridge.

## **4.2. Future Work**

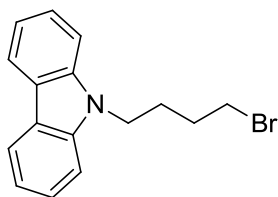
Studies for the optimization of the density of the biotinylated compound on gold surface are underway. In order to check the biospecificity of these biotinylated surfaces, model proteins like fibrinogen and lysozyme can be tested. These two proteins behave differently under the given experimental conditions. Fibrinogen is a large protein with molecular weight 340 kDa. Its pI is 5.5 and it is negatively charged under neutral buffer solutions. Lysozyme, on the other hand is a small and hard protein with molecular weight 14.7 kDa. It is positively charged in neutral buffer solutions since it has a pI 4.7. Moreover, the biotinylated carbazole can also be studied at the air-water interface using a Langmuir-Blodgett technique since they are amphiphilic in nature.

## **Appendices: $^1\text{H}$ and $^{13}\text{C}$ NMR**

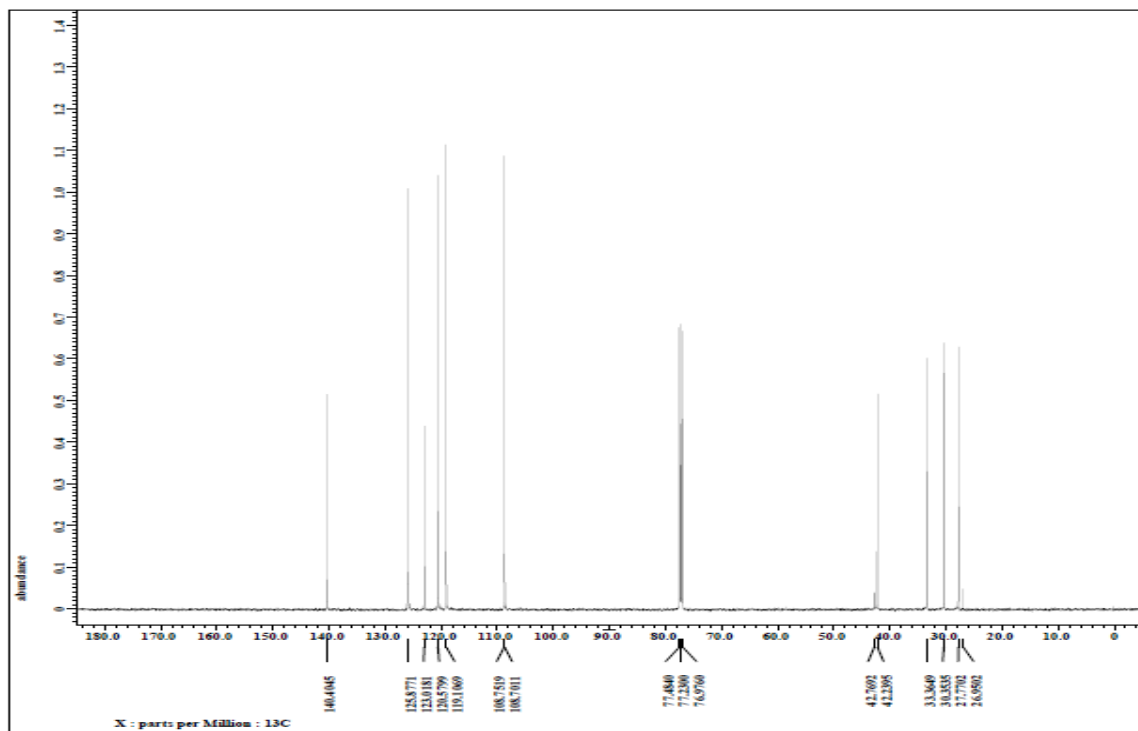




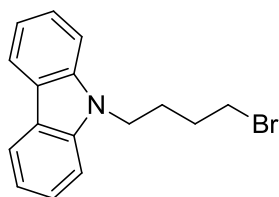
**A1.** 9-(4-Bromobutyl)-9H-carbazole



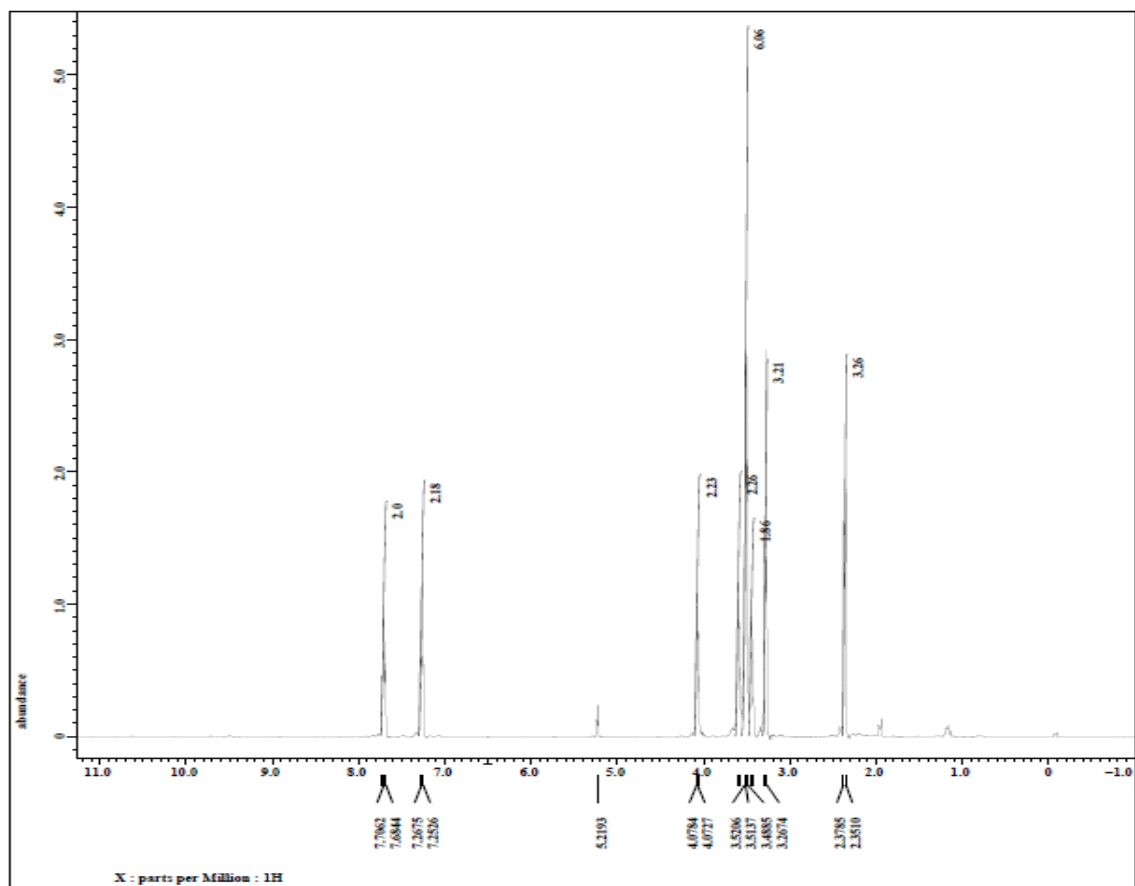
**1**



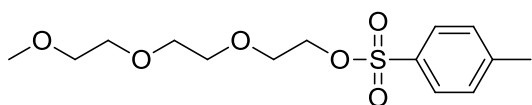
**A1.** 9-(4-Bromobutyl)-9H-carbazole



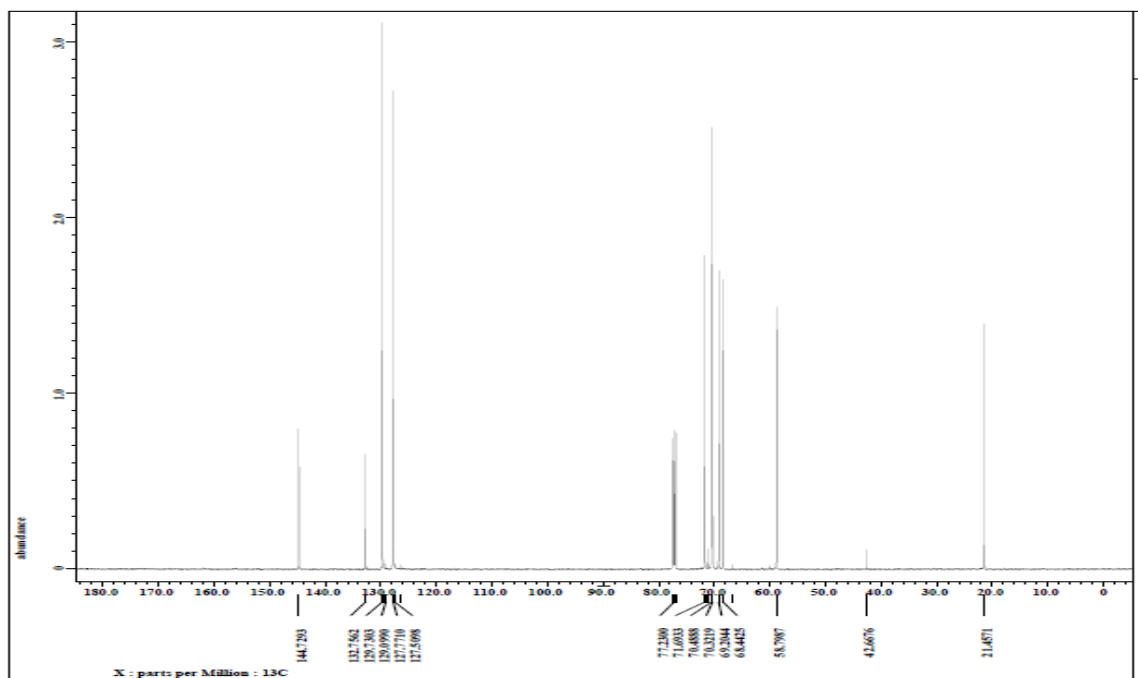
**1**



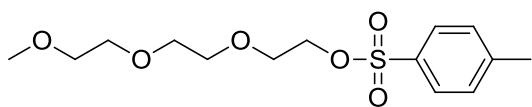
**A2.** Toluene-4-sulfonic acid-2-[2-(2-methoxyethoxy)-ethoxy]ethyl ester



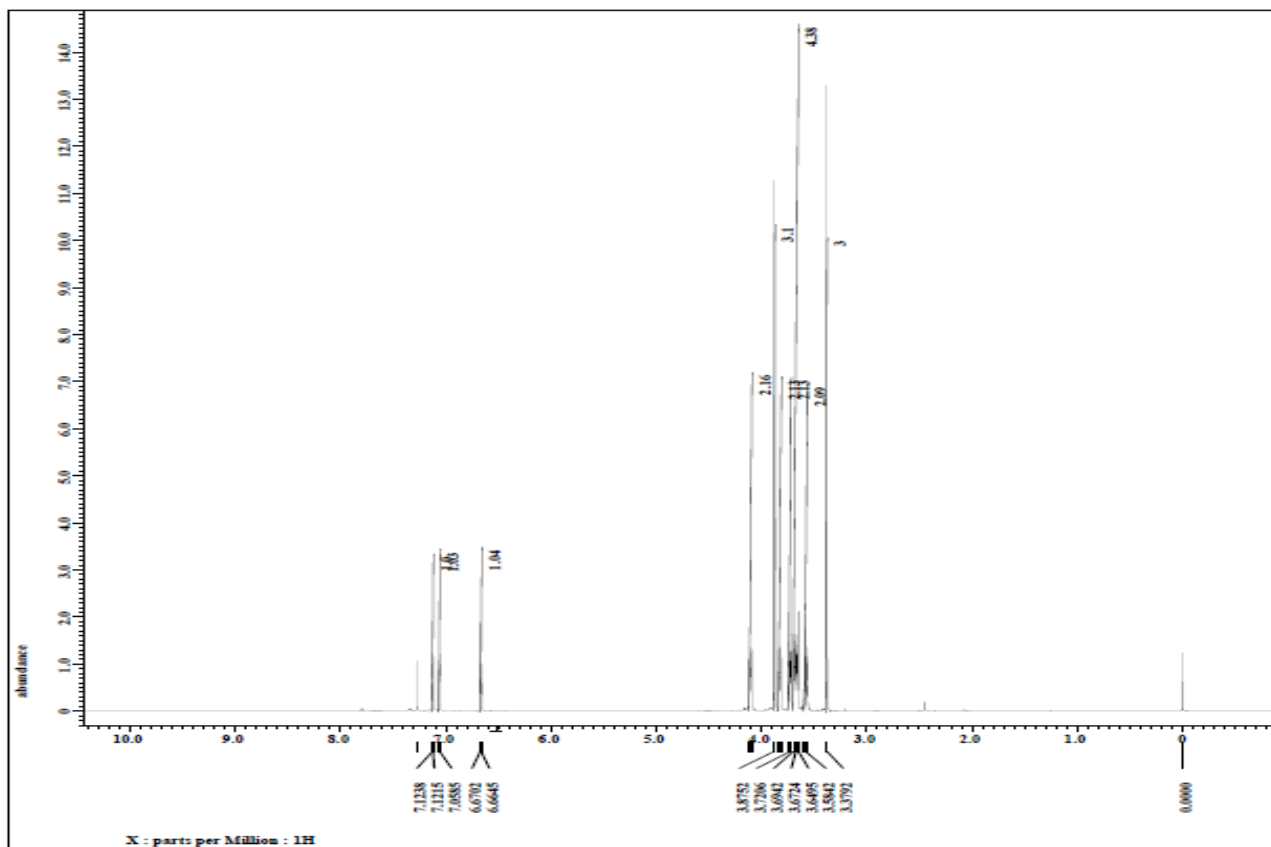
**2**



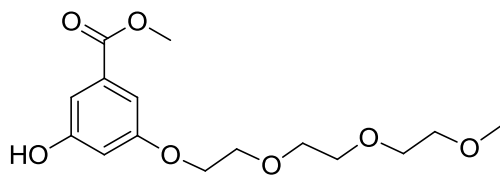
**A2. Toluene-4-sulfonic acid-2-[2-(2-methoxyethoxy)-ethoxy]ethyl ester**



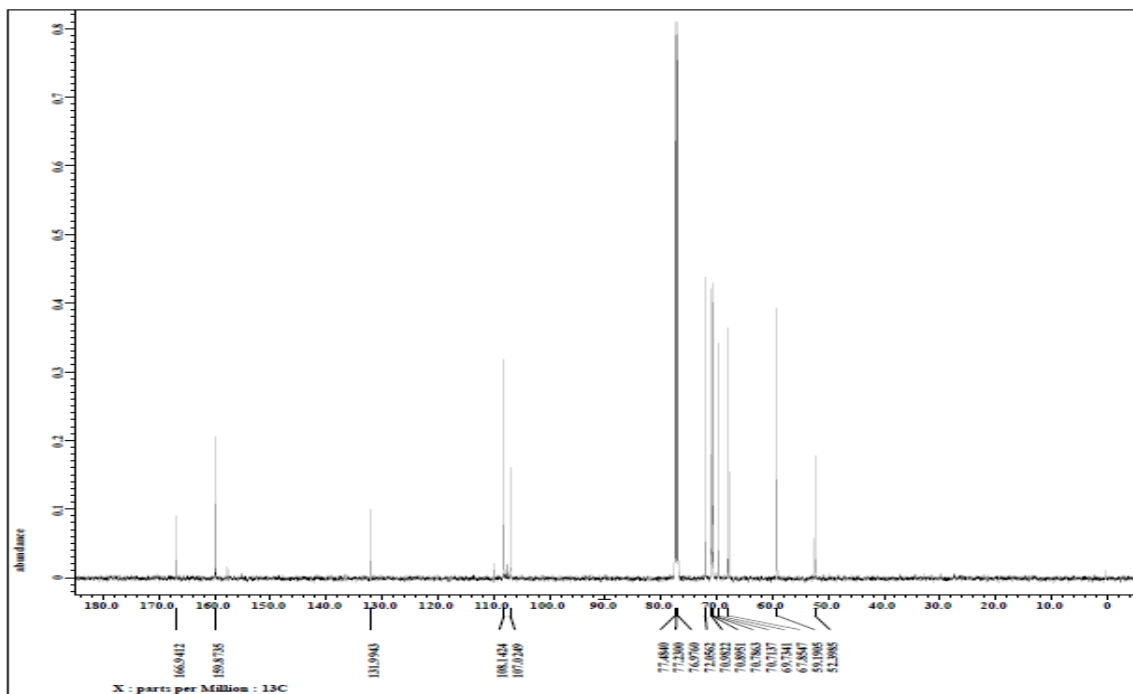
**2**



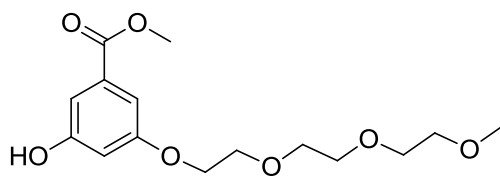
**A3.** Synthesis of 3-Hydroxy-5-{2-[2-(2-methoxyethoxy)ethoxy]ethoxy}benzoic acid methyl ester.



**3**

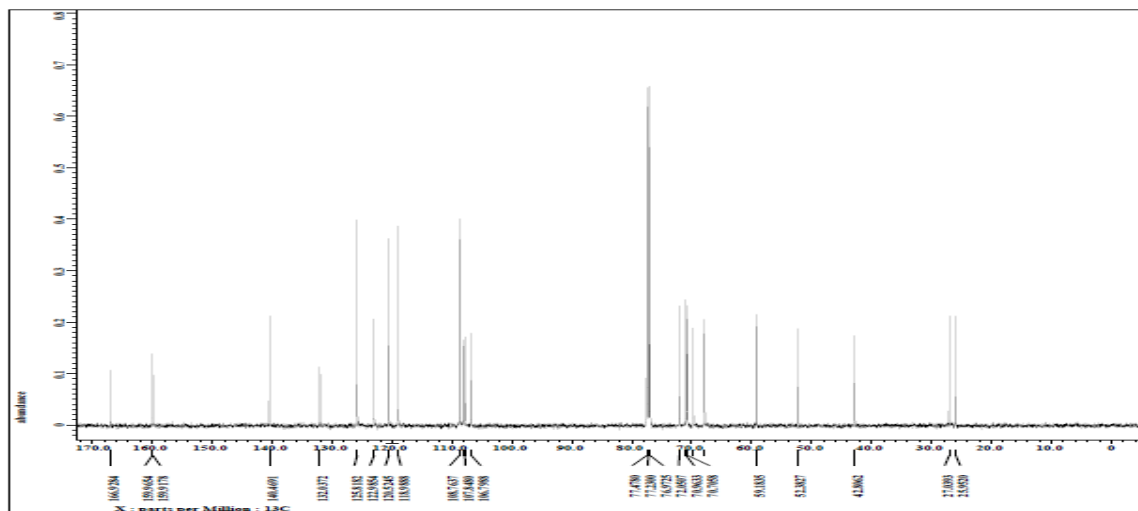


**A3.** Synthesis of 3-Hydroxy-5-{2-[2-(2-methoxyethoxy)ethoxy]ethoxy}benzoic acid methyl ester.

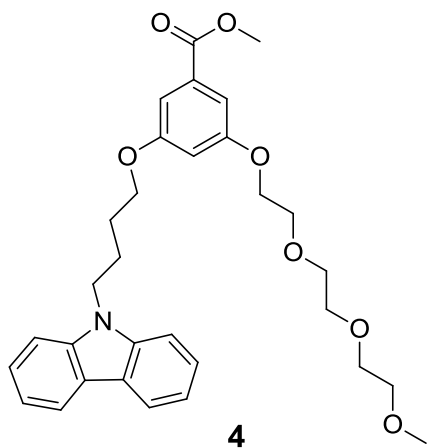


**3**

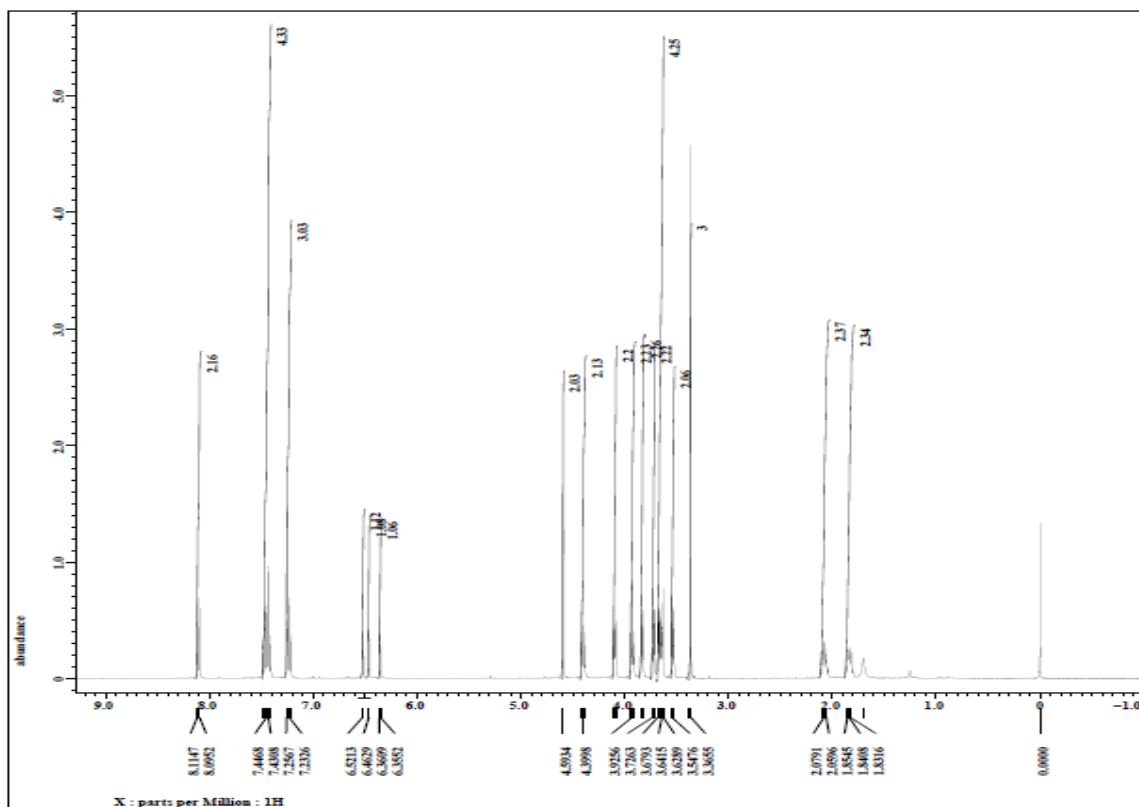




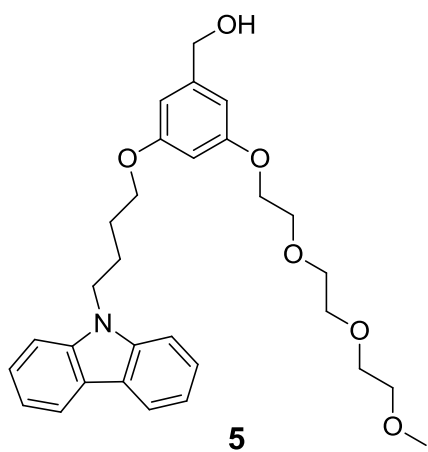
**A4.** (3-(4-Carbazol-9-yl-butoxy)-5-{2-[2-(2-methoxyethoxy)-ethoxy]-ethoxy}-benzoic acid methyl ester

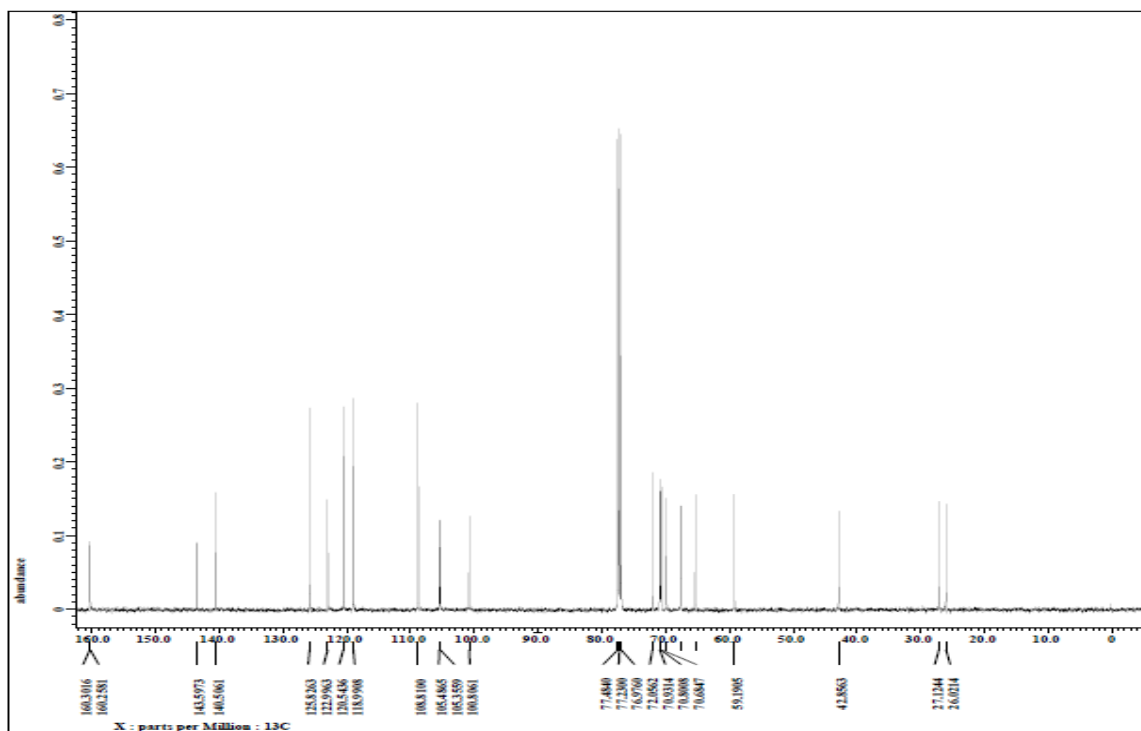




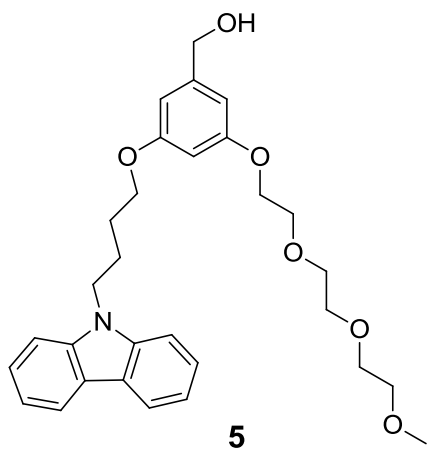


**A5.** (3-(4-Carbazol-9-yl-butoxy)-5-{2-[2-(2-methoxyethoxy)-ethoxy]-ethoxy}-phenyl)-methanol

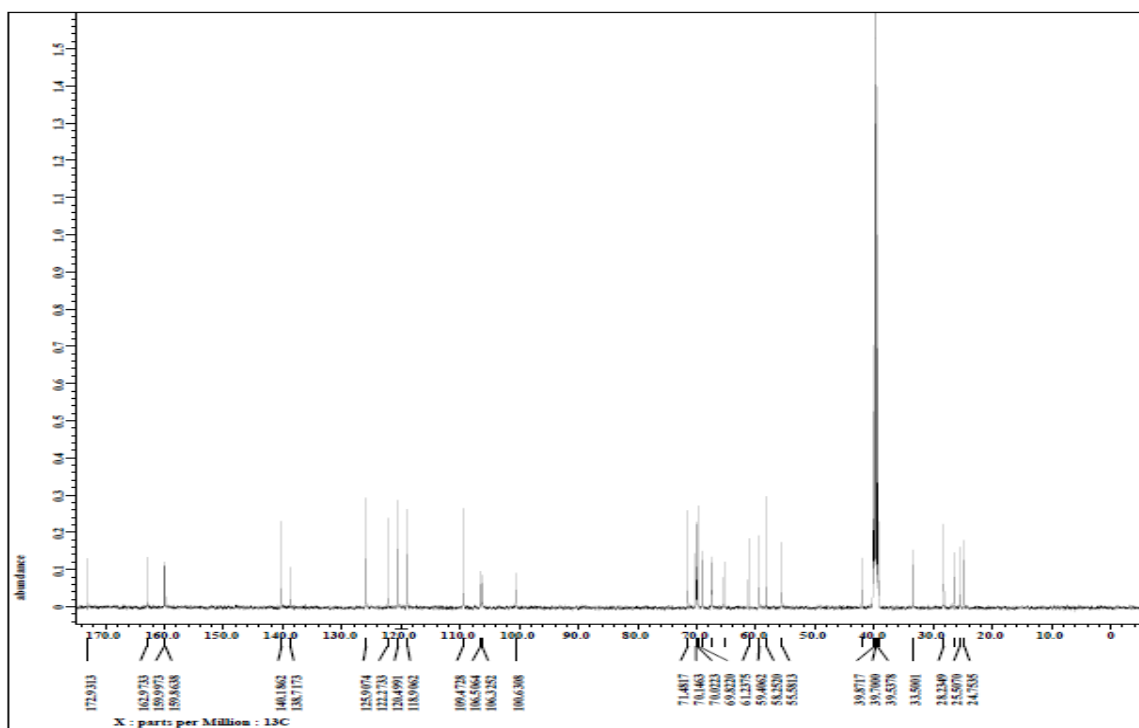




**A5.** (3-(4-Carbazol-9-yl-butoxy)-5-{2-[2-(2-methoxyethoxy)-ethoxy]-ethoxy}-phenyl)-methanol







**A6.** 5-(2-Oxo-hexahydro-thieno[3,4-d]imidazole-4-yl)-pentanoic acid 3-(4-carbazol-9-yl-butoxy)-5-{2-[2-(2-methoxyethoxy)-ethoxy]-ethoxy}-benzyl ester

